

# Jingfang Granules for Diabetic Wound Healing: Insights from Network Pharmacology and Experimental Validation

Rongrong Wang<sup>1,2,\*</sup>, Qian Wang<sup>1,2,\*</sup>, Mingfei Liu<sup>3,\*</sup>, He Xiao<sup>4</sup>, Guimin Zhang<sup>5,6</sup>, Jingchun Yao<sup>5,6</sup>, Ming Liu<sup>1,2</sup>

<sup>1</sup>Key Laboratory of Marine Drugs, Ministry of Education, School of Medicine and Pharmacy, Ocean University of China, Qingdao, 266003, People's Republic of China; <sup>2</sup>Laboratory for Marine Drugs and Bioproducts, Qingdao Marine Science and Technology Center, Qingdao, 266237, People's Republic of China; <sup>3</sup>School of Chinese Materia Medica, Tianjin University of Traditional Chinese Medicine, Tianjin, 301617, People's Republic of China; <sup>4</sup>Experimental Research Center, China Academy of Chinese Medical Sciences, Beijing, 100700, People's Republic of China; <sup>5</sup>State Key Laboratory of Integration and Innovation of Classic Formula and Modern Chinese Medicine, Lunan Pharmaceutical Group Co. Ltd., Linyi, 276005, People's Republic of China; <sup>6</sup>Linyi Key Laboratory for Immunopharmacology and Immunotoxicology of Natural Medicine, Lunan Pharmaceutical Group Co. Ltd., Linyi, 273400, People's Republic of China

\*These authors contributed equally to this work

Correspondence: Ming Liu; Jingchun Yao, Email [lmouc@ouc.edu.cn](mailto:lmouc@ouc.edu.cn); [yaojingchun@yeah.net](mailto:yaojingchun@yeah.net)

**Background:** Diabetic wounds are one of the most common complications of diabetes mellitus. Jingfang Granules (JFG), a combination of 11 herbs, has been clinically used for treating colds and the flu and for preventing various skin diseases.

**Purpose:** The present study was designed to evaluate the therapeutic effect of JFG on diabetic wounds and to elucidate the associated mechanisms.

**Methods:** JFG serum was prepared using Sprague-Dawley rats and the phytochemicals of JFG in the serum were identified using UHPLC-ESI-QE-Orbitrap-MS. A cell viability assay and cellular angiogenesis methods were performed to evaluate wound healing in vitro. Diabetic wounds were developed using streptozotocin-induced diabetic rats to investigate the efficacy of JFG on diabetic wounds in vivo. Network pharmacology analysis, molecular docking, and Western blot were performed to elucidate the potential mechanisms of JFG in diabetic wound healing.

**Results:** JFG serum attenuated H<sub>2</sub>O<sub>2</sub>-induced and high glucose-induced oxidative damage, significantly reduced lipopolysaccharide-induced upregulation of inflammatory cytokines, and promoted angiogenesis in vitro. In diabetic rats, JFG effectively promoted wound healing, reduced blood glucose and lipid levels, and alleviated oxidative stress and inflammation. A total of 56 phytochemicals were identified in the JFG serum. Six core targets (AKT1, EGFR, MAPK3, MAPK1, IL6, and TNF) and the PI3K-AKT and MAPK signaling pathways were identified by network pharmacology analysis, which were further validated by subsequent experimental methods.

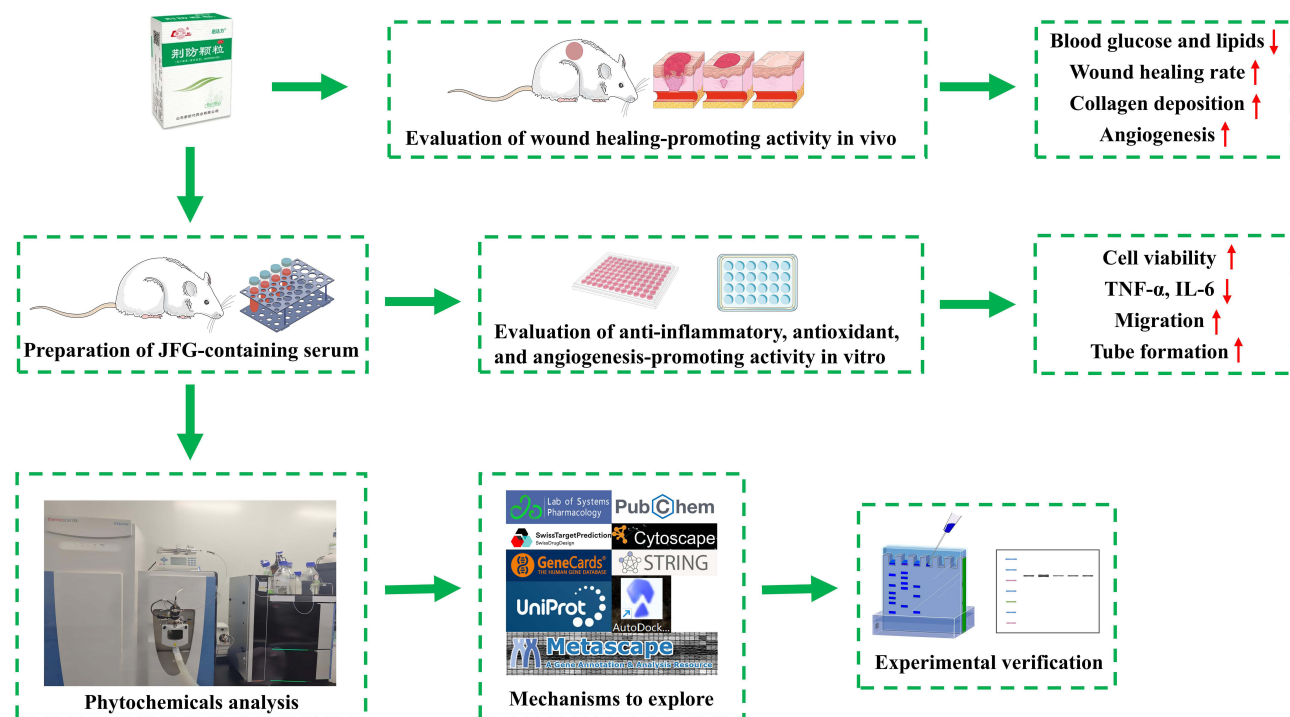
**Conclusion:** JFG could accelerate diabetic wound healing by alleviating oxidative damage, suppressing inflammation, promoting angiogenesis, and regulating metabolic abnormalities, with involvement of the PI3K-AKT and MAPK signaling pathways.

**Keywords:** jingfang granules, diabetic wounds, network pharmacology, MAPK, PI3K-AKT

## Introduction

Diabetic wounds, characterized by inherent chronic nonhealing wounds, are one of the most serious complications of diabetes and severely affect patients' quality of life. The pathogenesis of diabetic wounds has not been fully elucidated, with current consensus positing multifactorial determinants encompassing neuropathy, vascular disease, excessive oxidative stress, inflammation and impaired angiogenesis.<sup>1-3</sup> Inducing angiogenesis, decreasing excessive oxidative stress, reducing high levels of blood glucose, and regulating inflammation are recognized as key factors in controlling diabetic wounds. Current diabetic wounds therapies face critical limitations. Four FDA-approved biological products (Becaplermin, Dermagraft,

## Graphical Abstract



Apligraf, Integra Dermal Regeneration Template) are limited by high costs and inadequate efficacy.<sup>4-7</sup> Traditional methods like debridement, dressings, antimicrobial agents, and pressure offloading often fail to achieve healing, while prolonged antibiotics increase resistance risks. Emerging therapies, including skin grafts, tissue replacements, cytokines, and stem cells, face challenges such as cost barriers, safety concerns, and inconsistent efficacy.<sup>8</sup> Therefore, no recognized and effective drug is currently available, and safe and effective drugs for diabetic wounds need to be discovered urgently. Notably, since diabetic wounds are a chronic disease with a long course and extremely complex pathological mechanisms, it seems preferable to break through current therapeutic concepts and take a holistic view as the basis of the therapeutic strategy using traditional Chinese medicine, rather than “treating the head when there is a headache and treating the foot when there is a foot injury”.

Traditional Chinese medicine formulations exhibit multifaceted biochemical complexity, with their pharmacodynamic profiles demonstrating polypharmacological modulation, a therapeutic paradigm that intrinsically aligns with the multi-dimensional therapeutic requirements of pathophysiologically intricate disorders. For example, ON101, composed of active ingredients from *Plectranthus amboinicus* and *Centella asiatica*, has been approved by China’s NMPA in November 2023 to treat diabetic foot ulcers. It has a unique drug mechanism, regulating macrophages in diabetic wounds that are imbalanced due to high blood glucose, improving inflammation, promoting tissue repair, and finally achieving complete wound healing.<sup>9</sup> Besides, several herbal extracts have been proved to accelerate the healing of diabetic wounds, for example, *Teucrium polium* hydroethanolic extract A, *Cinnamomum* hydroethanolic extract, and *Quercus infectoria gall* extract promoted diabetic wound healing by shortening the inflammatory period or increasing antioxidant capacity.<sup>10</sup> Thus, traditional herbal medicines or compound prescriptions of natural origin have great potential and advantages in the treatment of diabetic wounds.<sup>10</sup>

Jingfang Granules (JFG) is a Chinese patent medicine derived from JingFangBaiDu San, an ancient herbal formula prescribed to treat the onset of sore, carbuncle, skin ulcer and “dry ringworm” (psoriasis) since the Ming dynasty. Currently, in clinical practice, JFG is mainly used for the flu, head and body pain, cold and fever, nasal congestion and runny nose.<sup>11</sup> JFG is composed of 11 herbs, including *Nepeta cataria* L. (Jing Jie), *Saposhnikovia divaricata* (Turcz. ex

Ledeb). Schischk. (Fang Feng), *Heracleum hemsleyanum* Diels (Du Huo), *Bupleurum chinense* DC. (Chai Hu), *Kitagawia praeurptora* (Dunn) Pimenov (Qian Hu), *Poria cocos* (Schw). Wolf (Fu Ling), *Platycodon grandiflorum* (Jacq). A. DC. (Jie Geng), *Hansenia weberbaueriana* (Fedde ex H. Wolff) Pimenov & Kljuykov (Qiang Huo), *Conioselinum anthriscoides* (Chuan Xiong), *Citrus aurantium* L. (Zhi Qiao), *Glycyrrhiza uralensis* Fisch. ex DC. (Gan Cao). The major chemical constituents of JFG have been validated including scopoletin,<sup>12</sup> troxerutin,<sup>13</sup> hesperetin,<sup>14</sup> etc., exhibiting significant anti-inflammatory and antioxidant activities. The presence of multiple bioactive compounds in JFG has enabled the ongoing exploration of novel indications associated with inflammation and oxidative stress, including acute kidney injury,<sup>15</sup> acute myocardial infarction,<sup>16</sup> acute pulmonary inflammation<sup>11</sup> and cold-dampness syndrome.<sup>17</sup> Moreover, JFG is also effective in treating various skin diseases, such as drug-induced dermatosis,<sup>18</sup> acne,<sup>19</sup> psoriasis<sup>20</sup> and urticaria,<sup>21</sup> which are associated with the reduction of the inflammatory response. Unlike other traditional Chinese medicine formulas, JFG is a pungent-neutral formula and exhibits dual therapeutic properties encompassing both immunoenhancement and anti-inflammatory regulation.<sup>11,22</sup> Considering the aforementioned unique characteristics of JFG and its ability to modulate oxidative stress and inflammation, which are also the key pathological features of diabetic wounds, we hypothesized about the potential effect of JFG in the treatment of diabetic wounds, and selected JFG as the investigational agent to explore whether JFG could enhance diabetic wound healing.

In this study, we investigated the effects of JFG on diabetic wounds using a variety of cell models under oxidative or inflammatory conditions in vitro and in a streptozotocin (STZ)-induced diabetic rats wound healing model in vivo, focusing on regulating inflammation, oxidative stress, angiogenesis, and metabolic abnormalities. We then determined the phytochemical composition of JFG in the serum using UHPLC-ESI-QE-Orbitrap-MS. Furthermore, network pharmacology analysis, molecular docking, and Western blot experimental validation were integrated to elucidate the possible mechanisms of JFG in diabetic wounds treatment.

## Materials and Methods

### Reagents and Drugs

JFG (Batch Number: 8022202002) was provided by Shandong New Time Pharmaceutical Co. Ltd. (Linyi, China), and was manufactured in strict compliance with the Chinese Pharmacopoeia (2020) and the Good Agricultural Practice for Chinese Crude Drugs standards. Its quality was validated through method verification and continuous stability monitoring, enabling full-process quality control from raw materials to finished products while ensuring batch-to-batch consistency. STZ was purchased from Beijing Solarbio Science and Technology Co. Ltd. (Beijing, China). Kits for tumor necrosis factor- $\alpha$  (TNF- $\alpha$ ) and interleukin-6 (IL-6) were obtained from Dakewe Biotech Co. Ltd. (Shenzhen, China). Glucose assay kits with O-toluidine, malondialdehyde (MDA), superoxide dismutase (SOD), oxidized glutathione (GSSG) and lipopolysaccharide (LPS) were obtained from Beyotime Biotechnology (Shanghai, China). Kits for the lactic acid assay, myeloperoxidase (MPO), triglyceride (TG), and total cholesterol (T-CHO) were supplied by Nanjing Jiancheng Bioengineering Institute (Nanjing, China). Antibodies against Protein Kinase B (AKT), phosphorylated AKT (p-AKT), Extracellular Signal-Regulated Kinase 1 and 2 (ERK1/2), phosphorylated ERK1/2 (p-ERK1/2), c-Jun N-terminal Kinase (JNK), phosphorylated JNK (p-JNK), and phosphorylated p38 Mitogen-Activated Protein Kinase (p-P38) were purchased from Cell Signaling Technology (Danvers, MA, USA). Antibodies against GAPDH and Tubulin were obtained from Huaan Biotechnology Co. Ltd. (Hangzhou, China). Antibodies against p38 Mitogen-Activated Protein Kinase (P38), TNF- $\alpha$ , and Interleukin-1 beta (IL-1 $\beta$ ) were purchased from Santa Cruz Biotechnology (Dallas, TX, USA).

### Animals

Sprague-Dawley (SD) rats (male, 200–220 g) were purchased from Beijing Vital River Laboratory Animal Technology Co., Ltd. (Beijing, China). The rats were housed in a clean, dedicated room with temperature control at  $25 \pm 2^\circ\text{C}$ , relative humidity of  $50 \pm 5\%$ , and a 12 h alternating light and dark cycle, with free access to food and water. All animal procedures were approved by the Institutional Animal Care and Use Committee of Ocean University of China (OUC-SMP-2023-12-02).

## Preparation of JFG Serum and Blank Serum

JFG serum and blank serum were prepared according to previously established protocols.<sup>20,22</sup> Briefly, SD rats (6 weeks old) were divided into 2 groups ( $n = 6$  per group): a blank serum group (rats received an equal amount of physiological saline as the JFG serum group) and a JFG serum group (10 g/kg/d). JFG was administered by gavage for 4 consecutive days, and blood samples were collected from the abdominal aorta of rats under anesthesia 1 h after the last dose, left to stand for 2 h, and then centrifuged for 15 min at 3000 rpm. The supernatant was inactivated at 56°C for 30 min, followed by filtration through a 0.22  $\mu\text{m}$  membrane to remove bacteria, aliquoted, and stored at  $-80^{\circ}\text{C}$  for subsequent experiments.

## Cell Culture

The immortalized human keratinocyte cell line HaCaT cells, human umbilical vein endothelial cells (HUVECs) and Raschke's Abelson murine leukemia virus-induced tumor 264.7 (RAW264.7) cells were obtained from the China Center for Type Culture Collection (CCTCC). Cells were cultured in DMEM medium (Senrui, Zhejiang, China) containing 10% fetal bovine serum (FBS) and 1% penicillin/streptomycin in a humidified incubator at 37°C with 5%  $\text{CO}_2$ .

## Cell Viability Assay

The 3-(4, 5-dimethylthiazol-2-yl)-2, 5-diphenyltetrazolium bromide (MTT) or sulforhodamine B (SRB) assays were used to determine cell proliferation ability according to previously described methods.<sup>23</sup> To detect the effect of JFG serum on cell proliferation, cells were seeded on 96-well plates and treated with JFG serum or blank serum for 48 h, followed by SRB assay. In the  $\text{H}_2\text{O}_2$ -induced oxidative damage model, cells were pretreated with blank serum or JFG serum for 48 h and then incubated with  $\text{H}_2\text{O}_2$  (200  $\mu\text{M}$  for HUVECs and 500  $\mu\text{M}$  for HaCaT cells) for 2 h followed by MTT assay. In high glucose (HG)-induced oxidative damage model, cells were treated with normal (25 mM) or HG (120 mM) medium plus blank serum or JFG serum for 48 h followed by SRB assay. For the MTT assay, MTT reagent was added and incubated, and DMSO was used to dissolve the formazan. The absorbance at 570 nm was detected using a microplate reader (Molecular Devices, San Jose, CA, USA). For the SRB assay, the supernatant was removed, trichloroacetic acid was added, followed by SRB reagent. Finally, the dyes produced in the living cells were solubilized, and the absorbance at 515 nm was measured.

## Inflammatory Cytokines Measurement and Glycolysis Analysis

Enzyme linked immunosorbent assay (ELISA) was used to determine the levels of pro-inflammatory cytokines in an LPS-induced model, as previously described.<sup>24</sup> Briefly, RAW264.7 cells were seeded in 24-well plates. The attached cells were treated with LPS (1  $\mu\text{g}/\text{mL}$ ) and different concentrations of JFG serum, with blank serum as the control. After incubation for 24 h, cell culture supernatants were obtained by centrifugation. The levels of TNF- $\alpha$ , IL-6, glucose, and lactic acid in the cell culture supernatant were detected using commercial kits according to the manufacturer's instructions.

## Wound Healing Assay

The effect of JFG serum on lateral migration was determined using an in vitro scratch wound assay, as previously described.<sup>25</sup> Cells were seeded in 24-well plates and incubated overnight. The next day, a scratch was made in the cell cultures using a 200  $\mu\text{L}$  pipette tip, followed by rinsing with PBS. Fresh medium containing blank serum or JFG serum was added, and cells were incubated for 24, 48, or 72 h. The scratches were photographed at each time point. The wound areas and the migration rate were assessed using the ImageJ software (ImageJ 1.53k), with migration rate calculated as:  $\text{Migration rate (\%)} = (\text{Area } 0 \text{ h} - \text{Area } t \text{ h}) / \text{Area } 0 \text{ h} \times 100$ .

## Transwell Migration Assay

The effect of JFG serum on the longitudinal migration of HUVECs was determined using an 8  $\mu\text{m}$  pore polycarbonate membrane transwell apparatus (Corning, New York, USA) as previously described.<sup>25</sup> First, the cells were placed on the transwell apparatus containing 1% FBS with blank or JFG serum and then placed together in the lower chamber

containing 10% FBS. After incubation, the membranes were washed and the cells were stained with crystal violet. Excess dye was removed from the upper surface of the membranes. Images were taken from randomly selected fields of the lower surface. Then, the crystal violet dye was dissolved in acetic acid, and absorbance was measured at 570 nm.

## Tube Formation Assay

Matrigel™ matrix (Mogengel, Xiamen, China) was used to determine the pro-angiogenic activity of the JFG serum, following a modified protocol.<sup>25</sup> First, pre-cooled Matrigel was added to a 96-well plate (50 µL/well) and allowed to solidify in an incubator at 37°C. Subsequently, a suspension of HUVECs ( $1.0 \times 10^4$  cells/well) containing blank serum or JFG serum was added on top of the matrigel. After incubation, tube formation in each well was recorded under a microscope and analyzed using ImageJ software (ImageJ 1.53k).

## JFG Treatment and Diabetic Wound Healing Assay

The rats were randomly divided into 4 groups (n = 6 per group): control, model, JFG-1 g/kg, and JFG-2 g/kg. The experimental timeline consisted of two phases: (1) a 9-day pre-treatment period for daily drug administration and induction of diabetes in rats prior to wound creation, and (2) a 14-day post-wounding observation period to monitor wound healing progression. More specifically, after 4 days of pre-administration, on day 5, hyperglycemia was induced in rats by injecting 65 mg/kg STZ into fasted animals.<sup>26</sup> After 72 h, blood glucose levels were monitored on day 9, and rats with blood glucose above 16.67 mmol/L were selected for subsequent experiments, referencing to a previous study on wound preparation.<sup>3</sup> In brief, after anesthetizing the rats with 2% (w/v) pentobarbital (Sigma-Aldrich, St. Louis, MO, USA), their backs were shaved, followed by the creation of two full-thickness wounds of 2 cm in diameter on both sides using sterile scissors. The rats were administered JFG by gavage once daily for 23 consecutive days. At the same time, equal amounts of physiological saline were given to the control and model groups as negative control. Photographs of the wound area were taken on days 0, 8, 12, and 14 post-injury. The wound healing rate was calculated as follows: wound healing rate (%) = (wound area on day 0 – wound area on the target day)/ wound area on day 0 × 100.

The rats were sacrificed and tissues containing the wound site and surrounding normal skin were collected and equally divided into two parts. One part was fixed with 4% paraformaldehyde for subsequent histological analysis, and the other was used for Western blot assays.

## Histological Analysis

Masson's trichrome staining was performed to measure collagen deposition according to the manufacturer's protocol, and collagen deposition was quantified using the Aipathwell® software (Servicebio, China). To evaluate angiogenesis in the skin wound tissues of the rats, immunohistochemical staining for platelet endothelial cell adhesion molecule-1 (CD31) was conducted.<sup>25</sup> After staining, the sections were observed under a PANNORAMIC microscope (3DHISTECH Ltd., Budapest, Hungary). Microvascular density (number of microvessels per field of view area) was calculated using the CaseViewer2.4 (3DHISTECH Ltd., Budapest, Hungary).

## Detection of Biochemical Indicators and Lipids in Rat Serum

At the end of the experiment, after fasting the animals for 12 h, rats were sacrificed, and blood was collected from the abdominal aorta. The serum was separated, aliquoted and stored at –80°C for subsequent assays. The serum levels of SOD, MDA, GSSG, MPO, TG, and T-CHO were assessed according to the manufacturer's instructions provided with kits.

## Phytochemical Analysis of JFG in Serum

Rats were randomly assigned to either the control group (physiological saline, i.g.) or JFG group (n=6, 10 g/kg/d, i.g). The rats were treated for 4 successive days. Prior to the last dose, all rats were fasted for 12 h. Following oral administration, the rats were anesthetized with 2% (w/v) pentobarbital (Sigma-Aldrich, St. Louis, MO, USA), and blood samples were collected from the abdominal aorta. The phytochemicals of JFG in serum were determined using UHPLC-ESI-QE-Orbitrap-MS and the processing and analysis methods were based on a previous study.<sup>27</sup>

## Network Pharmacological Analysis of JFG Phytochemicals in Serum for Diabetic Wound Management

Network pharmacological analysis was adapted from prior protocols with minor modifications.<sup>11</sup> Target collection was performed using the TCMSP (<https://old.tcmsp-e.com/tcmsp.php>) and SwissTargetPrediction (<http://swisstargetprediction.ch/>) databases. All target gene names were normalized via the UniProt database (<https://www.uniprot.org/>) and “diabetic wounds” was searched in the Genecards database (<https://www.genecards.org/>). Genes related to diabetic wounds and target genes of JFG phytochemicals in serum were uploaded to the jvenn platform (<https://jvenn.toulouse.inrae.fr/app/example.html>) to obtain the intersection genes. The resultant intersecting gene targets were imported into the STRING database platform (<https://string-db.org/>) to obtain a protein-protein interaction (PPI) network. The degree values of the target genes were analyzed using Cytoscape 3.8.0 software, to identify key target genes for determining the effects of JFG phytochemicals on diabetic wounds. These key target genes were imported into the Metascape database (<https://metascape.org/gp/index.html#/main/step1>) for Gene Ontology (GO) and Kyoto Encyclopedia of Genes and Genomes (KEGG) pathway enrichment analysis to identify the preliminary mechanisms involved in the alleviation of diabetic wounds by phytochemicals present in the serum. The top 20 pathways were selected as potential signaling mechanisms of JFG phytochemicals present in the serum for the treatment of diabetic wounds.

## Molecular Docking

Putative protein targets were selected based on PPI network analysis prioritizing node degree centrality and their pathophysiological relevance to diabetic wounds. The structures of AKT1 (PDB ID: 1UNQ), EGFR (PDB ID: 8A27), MAPK3 (PDB ID: 6GES), MAPK1 (PDB ID: 3SA0), IL6 (PDB ID: 1ALU) and TNF (PDB ID: 5UUI), were downloaded from the PDB database (<https://www.rcsb.org/>). The chemical structures of the JFG phytochemicals in the serum were obtained using the PubChem database (<https://pubchem.ncbi.nlm.nih.gov/>). Following pre-processing of their structures with PyMOL 2.3.0 software (<https://pymol.org/>), AutoDock Tools 1.5.7 (The Scripps Research Institute, CA, USA) was applied to identify the binding modes between the targets and JFG phytochemicals, and AutoDock Vina was employed to calculate the binding energies, with methods adapted from previous studies.<sup>11</sup> Binding affinity < -4.25 kcal/mol indicated binding activity, < -5 kcal/mol was considered good and < -7 kcal/mol was deemed strong.<sup>28</sup> Finally, the results were analyzed and visualized using PyMOL 2.3.0 and Discovery Studio 4.5.

## Western Blot Assay

Western blot assay was performed to validate the enriched signaling pathways and targets identified through network pharmacology, based on degree values and pathophysiological relevance to diabetic wounds. The skin tissues of each group were weighed and added to the lysate medium at a weight (mg) to volume ( $\mu$ L) ratio of 1:9. Skin tissue homogenates prepared under ice bath conditions to produce homogenates, centrifuged, and the supernatant was used for the bicinchoninic acid (BCA) assay. After measuring protein concentration, samples were boiled and denatured. Subsequently, proteins were separated via SDS-PAGE and transferred to NC membranes (Millipore, Billerica, MA, USA). The membranes were then blocked with skimmed milk, washed, and incubated overnight with the corresponding primary antibodies against AKT (1:2000), p-AKT (1:2000), ERK1/2 (1:2000), p-ERK1/2 (1:2000), JNK (1:2000), p-JNK (1:2000), p-P38 (1:2000), P38 (1:200), TNF- $\alpha$  (1:200) and IL-1 $\beta$  (1:200). After washing off the unbound primary antibodies, the next day, the membranes were incubated with horseradish peroxidase-conjugated secondary antibody (1:5000) for 1 h, washed again, and assayed using Tanon 5 imaging system (Tanon, Beijing, China).<sup>24</sup> Quantification of protein bands was conducted using ImageJ software (ImageJ 1.53k).

## Statistical Methods

GraphPad prism 8 (GraphPad Software, San Diego, CA, USA) was employed for statistical analysis. The data were expressed as mean  $\pm$  standard deviation (SD). Student's unpaired *t*-test was used for comparisons between two groups, and one-way ANOVA followed by Tukey's post hoc test was used for comparisons between multiple groups. In

experiments involving two independent variables, two-way ANOVA with Sidak's multiple comparisons test was applied for comparisons between multiple groups. A  $p$ -value  $< 0.05$  was considered of statistically significant.

## Results

### JFG Serum Ameliorates Oxidative Stress-Induced Cell Damage

In order to characterize the activity of JFG in vitro, we prepared drug-containing serum by the oral administration of JFG to rats. Since excessive oxidative stress is an important pathogenic mechanism in diabetic wounds, we investigated the cytoprotective effect of JFG serum in HaCaT cells and HUVECs utilizing an  $H_2O_2$ -induced oxidative damage model. The results showed that the selected concentrations of JFG serum were non-toxic (JFG serum vs blank serum,  $p > 0.05$ , Figure 1A and B), and could significantly alleviate  $H_2O_2$ -induced cell damage in HaCaT and HUVECs cell lines

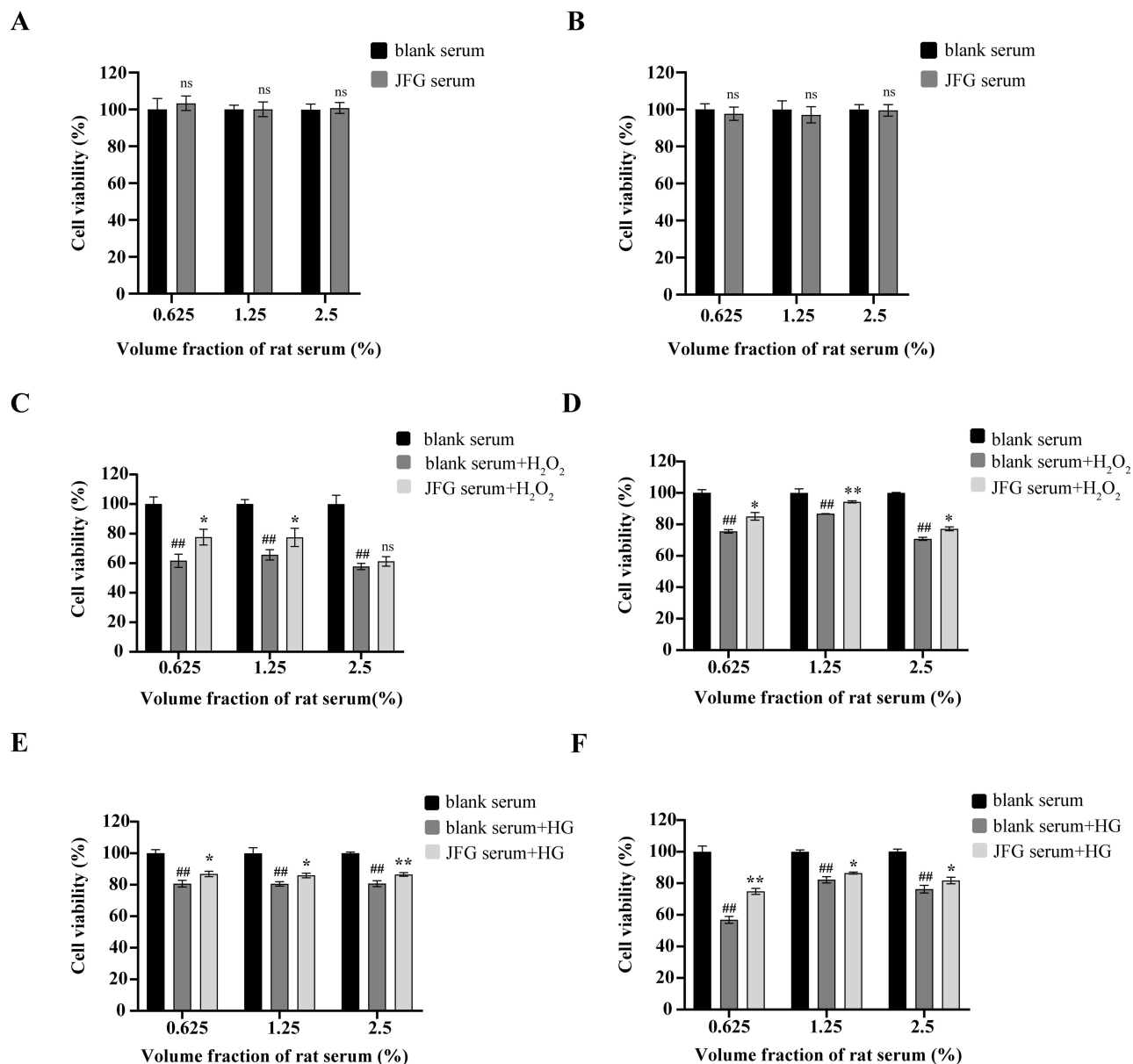


**Figure 1** Jingfang Granules (JFG) serum attenuates oxidative stress-induced cell damage. HaCaT cells (A) and HUVECs (B) were treated with JFG serum or blank serum, and cell viability was measured. Cells were treated with selected concentrations of JFG serum or blank serum, and then were exposed to  $H_2O_2$  for indicated time. Cell viability of HaCaT cells (C) and HUVECs (D) was detected.  $^{\#}p < 0.05$ ,  $^{\#\#}p < 0.01$  vs blank serum group;  $^*p < 0.05$ ,  $^{**}p < 0.01$  vs blank serum with  $H_2O_2$  group. JFG serum alleviated high glucose (HG)-induced cell damage. HaCaT cells (E) and HUVECs (F) were cotreated with HG and JFG serum or blank serum, and cell viability was assessed. Data are expressed as mean  $\pm$  SD of independent experiments,  $n=6$ .  $^{\#}p < 0.05$ ,  $^{\#\#}p < 0.01$  vs blank serum with normal glucose group;  $^*p < 0.05$ ,  $^{**}p < 0.01$  vs blank serum with HG group; "ns" indicates "not significant" ( $p > 0.05$ ).

(Figure 1C: 0.625 and 1.25% JFG serum+H<sub>2</sub>O<sub>2</sub> vs 0.625 and 1.25% blank serum+H<sub>2</sub>O<sub>2</sub>,  $p < 0.05$ ; 2.5% JFG serum+H<sub>2</sub>O<sub>2</sub> vs 2.5% blank serum+H<sub>2</sub>O<sub>2</sub>,  $p > 0.05$ ; Figure 1D: 0.625 and 2.5% JFG serum+H<sub>2</sub>O<sub>2</sub> vs 0.625 and 2.5% blank serum+H<sub>2</sub>O<sub>2</sub>,  $p < 0.05$ ; 1.25% JFG serum+H<sub>2</sub>O<sub>2</sub> vs 1.25% blank serum+H<sub>2</sub>O<sub>2</sub>,  $p < 0.01$ ). Hyperglycemia-induced oxidative stress exacerbates the risk of diabetic complications, including diabetic vasculopathy and diabetic wounds.<sup>29</sup> We then investigated the protective effect of JFG serum on cells under HG conditions. The results revealed that JFG serum afforded protection against HG-induced cell damage (Figure 1E: 0.625 and 1.25% JFG serum + HG vs 0.625 and 1.25% blank serum + HG,  $p < 0.05$ ; 2.5% JFG serum + HG vs 2.5% blank serum + HG,  $p < 0.01$ ; Figure 1F: 0.625% JFG serum + HG vs 0.625% blank serum + HG,  $p < 0.01$ ; 1.25 and 2.5% JFG serum + HG vs 1.25 and 2.5% blank serum + HG,  $p < 0.05$ ). These data indicate that JFG serum significantly mitigated the oxidative damage to HaCaT cells and HUVECs, which is beneficial for reducing the damage caused by hyperglycemia and oxidative stress to the epidermis and endothelium of blood vessels.

## JFG Serum Inhibits LPS-Stimulated Inflammation but Does Not Affect Glycolysis in RAW264.7 Cells

Considering that the persistent inflammation is another main contributor to non-healing diabetic wounds, we evaluated the anti-inflammatory effects of JFG serum in LPS-induced RAW264.7 cells. As shown in Figure 2A and B, pro-inflammatory cytokines IL-6 and TNF- $\alpha$  were significantly elevated by LPS (blank serum + LPS vs blank serum,  $p < 0.01$ ). Both 0.625 and 1.25% JFG serum reduced IL-6 and TNF- $\alpha$  levels elevated by LPS (IL-6: 0.625% JFG serum + LPS vs 0.625% blank serum +

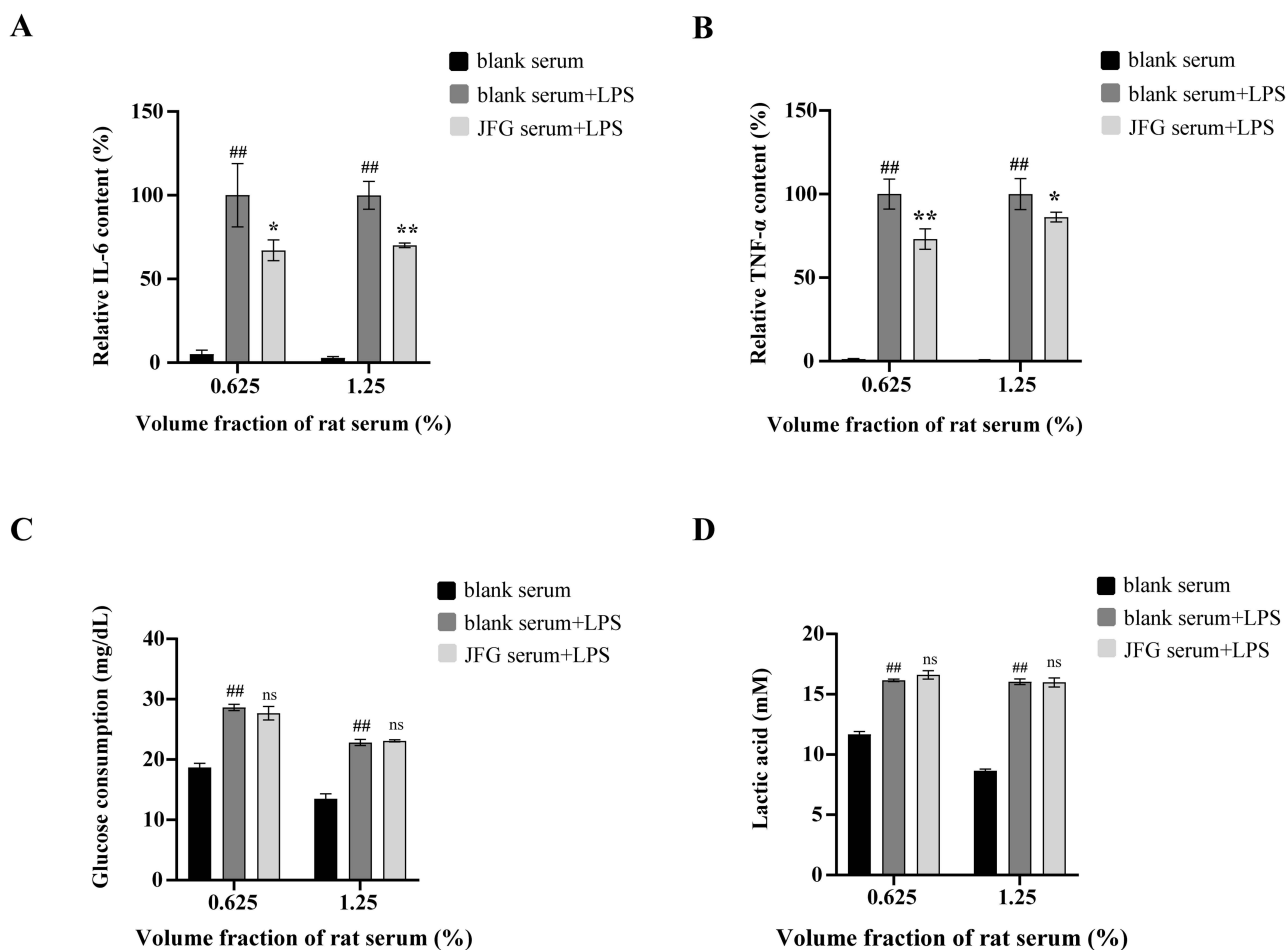


**Figure 2** JFG serum suppresses lipopolysaccharide (LPS)-induced inflammation in RAW264.7 cells. Effects of 0.625 and 1.25% JFG serum on the levels of interleukin-6 (IL-6) (A) tumor necrosis factor- $\alpha$  (TNF- $\alpha$ ) (B) glucose consumption (C) and lactic acid production (D). Data are expressed as mean  $\pm$  SD of independent experiments,  $n=6$ . ## $p < 0.01$  vs blank serum group; \* $p < 0.05$ , \*\* $p < 0.01$  vs blank serum with LPS group; "ns" indicates "not significant" ( $p > 0.05$ ).

LPS,  $p < 0.05$ ; 1.25% JFG serum + LPS vs 1.25% blank serum + LPS,  $p < 0.01$ ; TNF- $\alpha$ : 0.625% JFG serum + LPS vs 0.625% blank serum + LPS,  $p < 0.01$ ; 1.25% JFG serum + LPS vs 1.25% blank serum + LPS,  $p < 0.05$ ), indicating that JFG serum also has anti-inflammatory activity. Then, we detected the effects of JFG serum on glycolysis, aiming to explore its anti-inflammatory mechanisms. As shown in [Figure 2C](#) and [D](#), glycolysis was abnormally activated by LPS, manifested by increased glucose consumption and lactic acid production (0.625 and 1.25% blank serum + LPS vs 0.625 and 1.25% blank serum,  $p < 0.01$ ); however, JFG serum could not restore the increase in glycolysis under the present experimental conditions (0.625 and 1.25% JFG serum + LPS vs 0.625 and 1.25% blank serum + LPS,  $p > 0.05$ ), suggesting that JFG serum might inhibit LPS-induced inflammation through other mechanisms.

## JFG Serum Promotes Angiogenesis in HUVECs

Because of insufficient angiogenesis, the density of blood vessels and capillaries in diabetic wounds is reduced, resulting in a significant delay in wound closure in diabetic patients.<sup>30</sup> Therefore, we next investigated the effect of JFG serum on angiogenesis in HUVEC cellular model. First, we evaluated the effect of JFG serum on the migration ability of HUVECs through in vitro scratch wound and transwell assays. As shown in [Figure 3A–C](#), in the scratch wound assay, a significant promotion of wound healing was observed with the treatment of JFG serum in all selected concentrations compared to blank serum at both 24 and 48 h (24 h: 0.625, 1.25 and 2.5% JFG serum vs 0.625, 1.25 and 2.5% blank serum,  $p < 0.05$ ; 48 h: 0.625, 1.25 and 2.5% JFG serum vs 0.625, 1.25 and 2.5% blank serum,  $p < 0.01$ ). The same healing-promoting effect of JFG serum was also observed in an in vitro HaCaT cells wound healing assay ([Figure S1](#)). Consistently, the results of the transwell assay showed that the migration rate of HUVECs increased after JFG serum treatment when compared to blank serum ([Figure 3D](#) and [E](#): 0.625, 1.25 and 2.5% JFG serum vs 0.625, 1.25 and 2.5% blank serum,  $p < 0.05$ ).

Second, we evaluated the effect of JFG serum on tube formation by HUVECs seeded on matrigel cotreated with JFG serum or blank serum. Characteristic images of the tube formation in each group are shown in [Figure 3F](#). Quantitative measurements showed that the number of nodes increased to varying degrees after incubation with different concentrations of JFG serum compared with the blank serum group ([Figure 3G](#): 0.625, 1.25 and 2.5% JFG serum vs 0.625, 1.25 and 2.5% blank serum,  $p < 0.01$ ). Altogether, these results indicated that JFG serum could stimulate epidermal restoration and promote angiogenesis in vitro.

## JFG Accelerates Diabetic Wound Healing in Diabetic Rats

Encouraged by the potential of JFG to ameliorate oxidative stress, inflammation and angiogenesis in vitro, we further evaluated the diabetic wound healing activity and explored the mechanism of JFG using a STZ-induced diabetic rat model. The specific experimental procedure is shown in [Figure 4A](#). In brief, after 4-day pretreatment, on day 5, fasted rats received STZ to induce hyperglycemia. On day 9, rats with blood glucose  $>16.67$  mmol/L were selected to create dorsal wounds and were administered JFG orally for 23 consecutive days. As shown in [Figure 4B–D](#), on day 8 after injury, the wound healing rate in the model group was 62.3% when compared with 85.8% in the normal control group (Model group vs Control group,  $p < 0.01$ ); JFG treatment noticeably reduced the delayed wound healing triggered by the hyperglycemic state and increased the healing rate to 69.8 and 72.5% at doses of 1 and 2 g/kg, respectively (JFG-1 g/kg vs Model group,  $p > 0.05$ ; JFG-2 g/kg vs Model group,  $p < 0.05$ ). On day 12 after injury, the wound healing rate in the model group was 81.1% (Model group vs Control group,  $p < 0.01$ ), which increased to 91.9 and 90.4% when treated with 1 and 2 g/kg JFG, respectively (JFG-1 g/kg vs Model group,  $p < 0.01$ ; JFG-2 g/kg vs Model group,  $p < 0.01$ ). On day 14 after injury, the wound healing rate in the model group was 88.3% compared to 97.3% in the control group (Model group vs Control group,  $p < 0.01$ ), while the wound healing rates in the JFG groups were 96 and 95% in the low-dose and high-dose groups, respectively (JFG-1 g/kg vs Model group,  $p < 0.05$ ; JFG-2 g/kg vs Model group,  $p < 0.05$ ).

Collagen is an important component of granulation tissue and is indispensable in the wound healing process.<sup>3</sup> Our results showed that after the administration of JFG, there was significantly more collagen production in the JFG group compared to the model group (JFG-1 g/kg vs Model group,  $p < 0.01$ ; JFG-2 g/kg vs Model group,  $p < 0.01$ ), reflecting a superior wound healing status ([Figure 4E](#) and [F](#)). CD31 is a surface molecule of vascular endothelial cells. Our immunohistochemistry results showed that the proportion of CD31-positive endothelial cells was significantly higher in

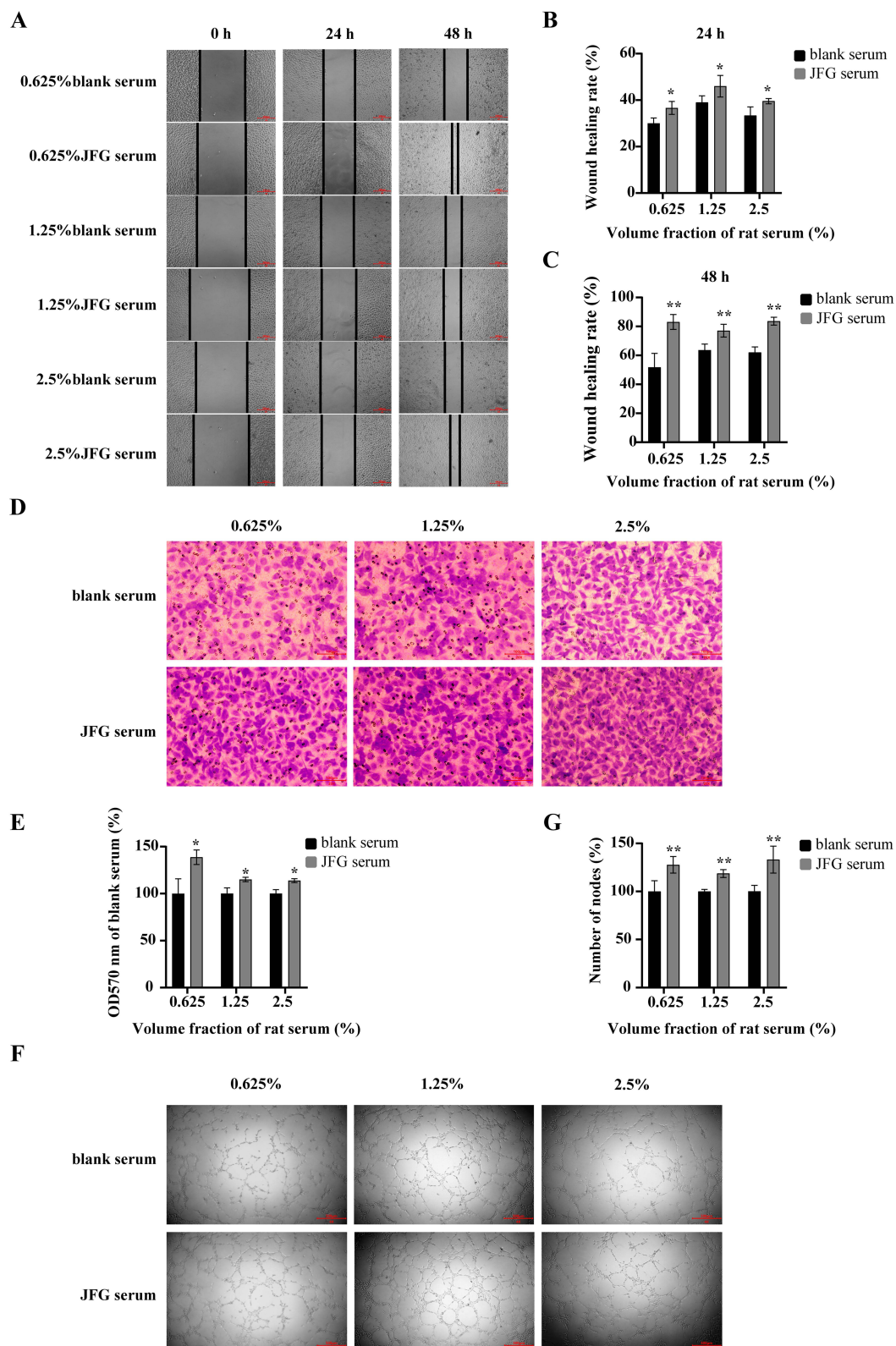


**Figure 3** JFG serum promotes angiogenesis in HUVECs. **(A)** Wound healing assay of HUVECs with blank serum or JFG serum incubated for 24 and 48 h (scale bars, 500  $\mu$ m). **(B and C)** Quantification of the migration rate of 24 and 48 h measured by ImageJ. **(D)** Effect of JFG serum on the vertical migratory capacity of HUVECs in the transwell assay (scale bars, 100  $\mu$ m). **(E)** Cells migrating to the lower chambers were stained with crystal violet and the absorbance was determined. **(F)** Effect of JFG serum on tube formation of HUVECs (scale bars, 500  $\mu$ m). **(G)** Number of nodes connecting individual complete capillaries. Data are expressed as mean  $\pm$  SD of independent experiments,  $n=6$ . \* $p < 0.05$ , \*\* $p < 0.01$  vs blank serum group; “ns” indicates “not significant” ( $p > 0.05$ ).

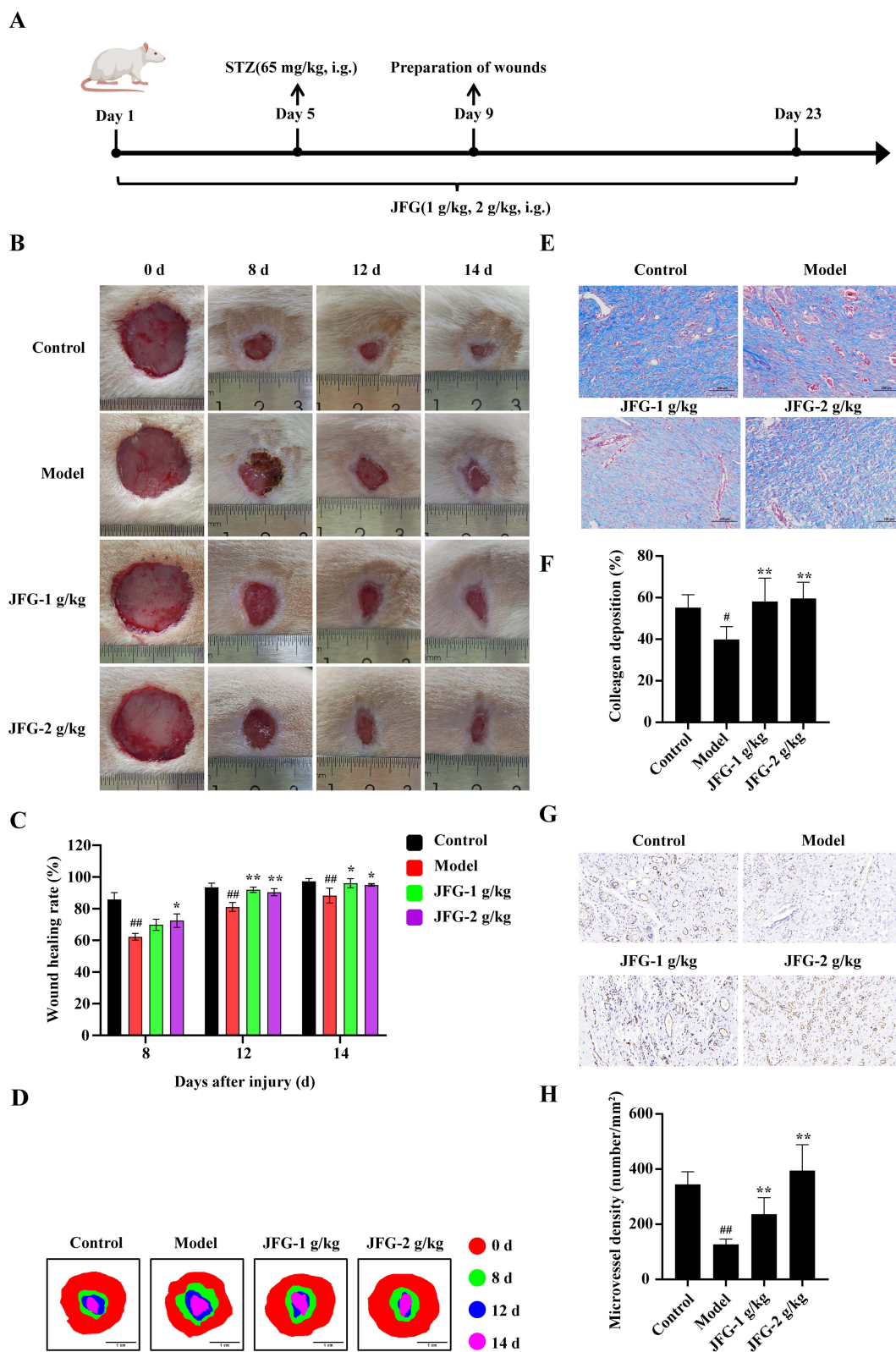


**Figure 4** JFG speeds wound healing in diabetic rats. **(A)** Schematic diagram of the experimental procedure. **(B)** Photographs of wounds on day 0, 8, 12, and 14 after injury. **(C)** Wound healing rate of each group on day 0, 8, 12, and 14 after injury. **(D)** Trace of wound closure in each group on day 0, 8, 12, and 14 after injury. Scale bars, 1 cm. **(E)** Collagen deposition of wound tissues on day 14 after injury. Scale bars, 100  $\mu$ m. **(F)** Masson trichrome staining was quantified by Aipathwell<sup>®</sup> software. **(G)** Immunohistochemical staining of platelet endothelial cell adhesion molecule-1 (CD31) in wound tissues on day 14 after injury. Scale bars, 20  $\mu$ m. **(H)** Histograms show the microvessel density of each group. Data are expressed as mean  $\pm$  SD of independent experiments,  $n=6$ . <sup>#</sup> $p < 0.05$ , <sup>##</sup> $p < 0.01$  vs control group; <sup>\*</sup> $p < 0.05$ , <sup>\*\*</sup> $p < 0.01$  vs model group; “ns” indicates “not significant” ( $p > 0.05$ ).

the JFG-treated group than that in the model group (Figure 4G–H, JFG-1 g/kg vs Model group,  $p < 0.01$ ; JFG-2 g/kg vs Model group,  $p < 0.01$ ), further suggesting that JFG could promote angiogenesis in wound tissues and accelerate diabetic wound healing in vivo.

## JFG Alleviates Metabolic Abnormalities, Excessive Oxidative Stress and Inflammation in Diabetic Rat Wounds

High blood glucose is responsible for delayed wound healing in diabetic patients.<sup>31</sup> Constituents of JFG, such as *Saposhnikovia divaricata* (Turcz. ex Ledeb). Schischk. (Fang Feng), *Conioselinum anthriscoides* (Chuan Xiong), *Poria cocos* (Schw). Wolf (Fu Ling) have been reported to reduce blood glucose levels and ameliorate the complications of diabetes mellitus.<sup>32</sup> We then investigated the effect of JFG on blood glucose levels in rats. As shown in Figure 5A and B, the model group showed significant weight loss (Figure 5A: Model group vs Control group,  $p < 0.01$ ) and higher blood glucose levels (Figure 5B: Model group vs Control group,  $p < 0.01$ ) after STZ administration compared to the control group. However, JFG treatment significantly reduced STZ-induced glycemic elevation in the high-dose group on days 16, 20, and 23 (Figure 5B: JFG-2 g/kg vs Model group,  $p < 0.05$ ) and significantly alleviated hyperglycemia-induced weight loss in both dose groups (Figure 5A: JFG-1 g/kg vs Model group,  $p < 0.01$ ; JFG-2 g/kg vs Model group,  $p < 0.01$ ). As shown in Figure 5C and D, the model group exhibited significantly higher levels of TG and T-CHO than the control group (Model group vs Control group,  $p < 0.01$ ), which were effectively reversed by JFG after 23 days of intervention (Figure 5C: JFG-1 g/kg vs Model group,  $p < 0.01$ ; JFG-2 g/kg vs Model group,  $p < 0.01$ ; Figure 5D: JFG-1 g/kg vs Model group,  $p > 0.05$ ; JFG-2 g/kg vs Model group,  $p < 0.01$ ) suggesting that JFG exhibited good performance in regulating blood lipids. Furthermore, we found that JFG treatment effectively alleviated oxidative stress in diabetic rats, as manifested by an increase in SOD activity and a decrease in MDA, MPO, and GSSG (Figure 5E–H: JFG-1 g/kg vs Model group,  $p > 0.05$ ; JFG-2 g/kg vs Model group,  $p < 0.05$ ). Diabetic wounds tend to stagnate during the inflammatory phase due to persistent chronic inflammation.<sup>33</sup> In our study, we found that the levels of TNF- $\alpha$  and IL-1 $\beta$  were higher in the skin wounds of diabetic rats compared to those of normal rats, and the levels of these two pro-inflammatory cytokines were significantly reduced with JFG treatment (Figure 5I–K: TNF- $\alpha$ : JFG-1 g/kg vs Model group,  $p < 0.01$ ; JFG-2 g/kg vs Model group,  $p < 0.01$ ; IL-1 $\beta$ : JFG-1 g/kg vs Model group,  $p < 0.05$ ; JFG-2 g/kg vs Model group,  $p < 0.01$ ), suggesting that JFG could alleviate the inflammatory state of diabetic wounds in vivo and thus accelerated diabetic wound healing. Overall, these results indicated that JFG attenuates metabolic aberrations, oxidative stress, and inflammation to accelerate diabetic wound healing in vivo.

## Identification of the Phytochemicals of JFG in Serum

To explore the active compounds in JFG serum and the potential mechanisms of JFG in the treatment of diabetic wounds, the phytochemicals of JFG in serum were identified using UHPLC-ESI-QE-Orbitrap-MS. As shown in Figure 6 and Table 1, 56 serum prototypes of JFG were analyzed and identified. Among them, 5 constituents belonged to coumarins, 14 to organic acids, 1 to lignans, 3 to flavonoids, 1 to amino acids, 6 to phenylpropanoids, 4 to phthalides, 2 to aldehydes, 6 to esters, 2 to aromatic ketones, 3 to terpenoids, 1 to monoterpene ketones, 1 to saccharides, 7 to other compounds. Most of these compounds have been considered to exhibit antioxidant, anti-inflammatory activity, or both.<sup>12–14</sup>

## Network Pharmacological Analysis of Phytochemicals of JFG in Serum for the Treatment of Diabetic Wounds

Next, network pharmacological analysis was performed, and 642 non-repetitive corresponding target protein genes were obtained from the TCMSP and SwissTargetPrediction databases. Detailed information regarding the 642 targets is provided in Table S1. Genes relevant to diabetic wounds were obtained from the GeneCards database, and 1409 target genes of diabetic wounds are collected in Table S2. As shown in Figure 7A, based on Tables S1 and S2, 241 intersecting genes were presented via a Venn diagram. Subsequently, to analyze protein interactions, these 241 intersecting genes were imported into the STRING database and Cytoscape 3.8.0 software for network analysis. As shown in Figure 7B, a PPI network was constructed, which revealed high combined scores for AKT1, EGFR, MAPK3, MAPK1, IL6, and

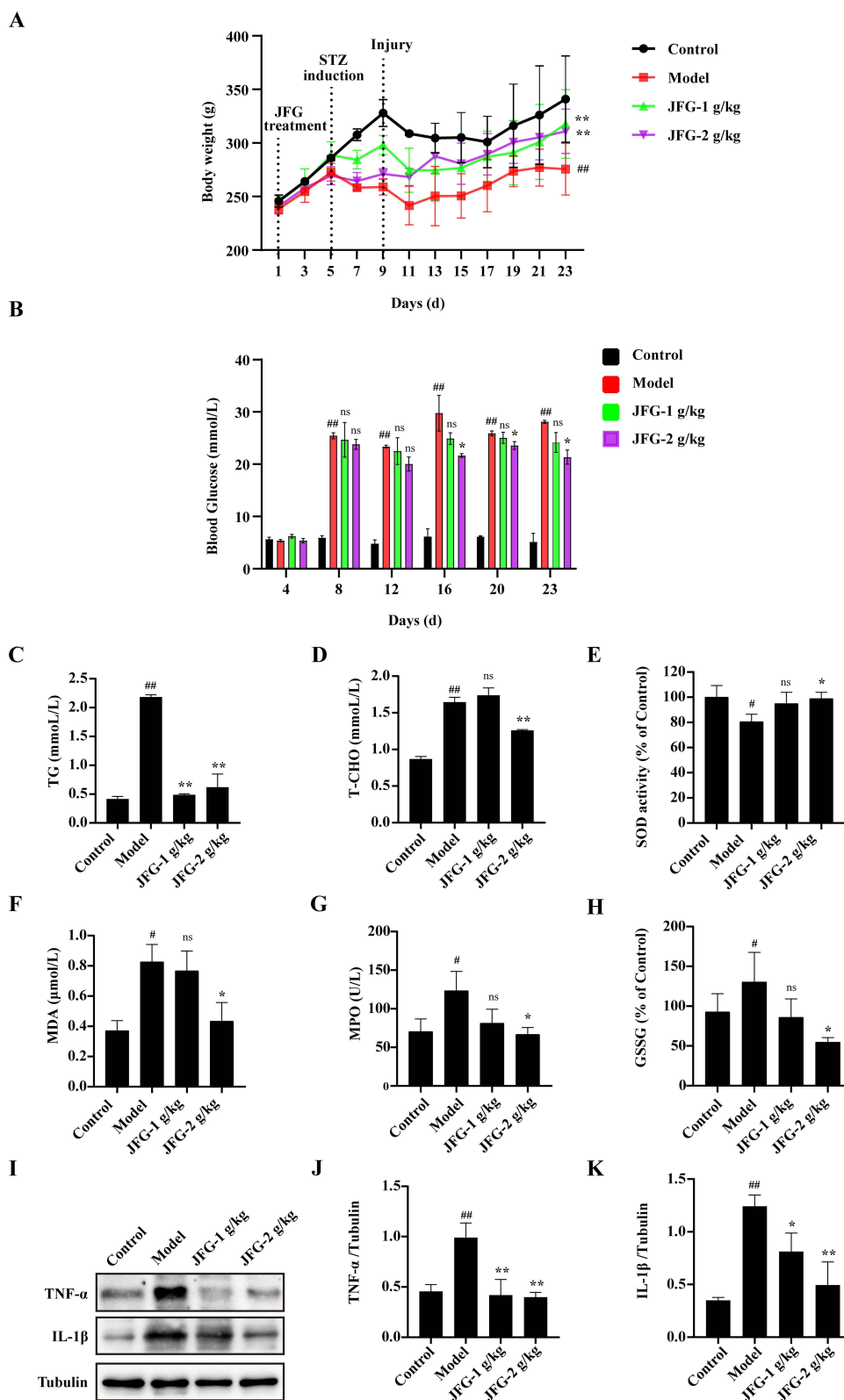


**Figure 5** JFG alleviates metabolism abnormalities, excessive oxidative stress and inflammation in diabetic rats. JFG was administered by gavage to diabetic rats and the serum was carefully separated. Changes in body weight (**A**) blood glucose (**B**) triglyceride (TG) (**C**) and total cholesterol (T-CHO) (**D**) after JFG treatment are shown. The serum levels of superoxide dismutase (SOD) (**E**), malondialdehyde (MDA) (**F**), myeloperoxidase (MPO) (**G**) and oxidized glutathione (GSSG) (**H**) were measured using indicated kit. (**I–K**) Western blot analysis of TNF- $\alpha$  and interleukin-1 beta (IL-1 $\beta$ ) in the wound tissues of diabetic rats. Data are expressed as mean  $\pm$  SD.  $^{##}p < 0.05$ ,  $^{###}p < 0.01$  vs control group;  $^{*}p < 0.05$ ,  $^{**}p < 0.01$  vs model group; “ns” indicates “not significant” ( $p > 0.05$ ).

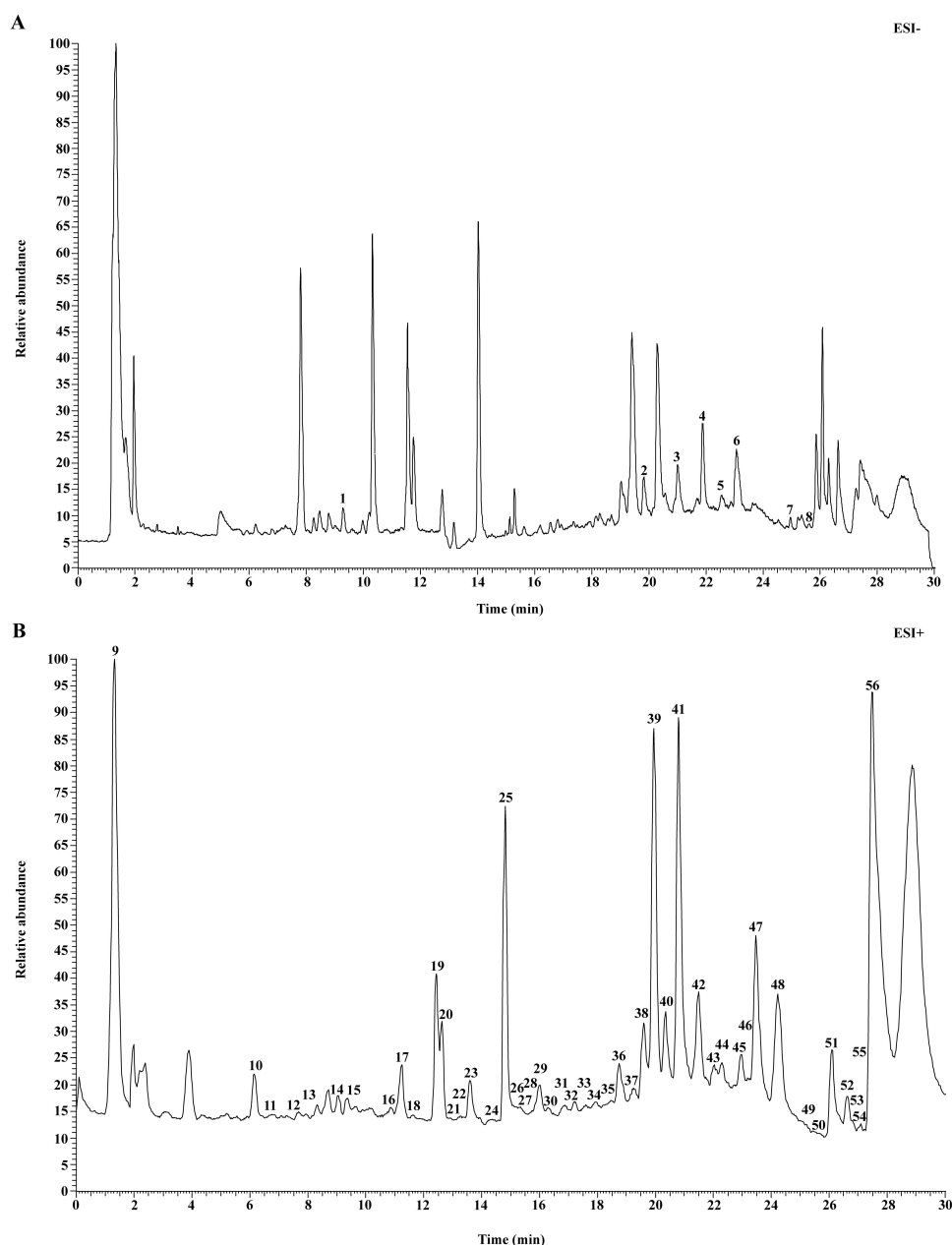


**Figure 6** Total ion chromatogram of JFG phytochemicals absorbed into rat serum after oral administration of 10 g/kg/d for 4 consecutive days. **(A)** Negative ion mode. **(B)** Positive ion mode.

TNF, indicating that JFG might achieve its therapeutic effects through multiple targets and multiple mechanisms. GO taxonomic enrichment analysis showed that key target genes were involved in the regulation of a variety of molecular functions, biological processes, and cellular components. The cellular components were mainly related to the transcription regulator complex, focal adhesion, receptor complex, etc. Biological process analysis included the positive regulation of phosphorylation, positive regulation of cell migration, response to oxidative stress, etc. Molecular functional analysis included DNA-binding transcription factor binding, phosphatase binding, cytokine receptor binding, etc. (Figure 7C). The results of KEGG signaling pathway analysis showed that the PI3K-AKT and MAPK signaling pathways might participate in the treatment of diabetic wounds by phytochemicals of JFG in the serum (Figure 7D).

**Table I** The Detected Ion Chromatogram of Phytochemicals in JFG Serum

No.	T <sub>R</sub> (min)	m/z		Ion Mode	ppm (10 <sup>-6</sup> )	Identification	Formula	Attribution	Classification
		Measured	Calculated						
1	9.29	262.0837	261.07643	ESI-	-1.6	Vaginidiol	C <sub>14</sub> H <sub>14</sub> O <sub>5</sub>	g	Coumarins
2	19.85	256.23904	255.23176	ESI-	-4.66	Palmitic acid	C <sub>16</sub> H <sub>32</sub> O <sub>2</sub>	a,b,c,d,f,g,h,j	Organic acids
3	21.01	282.25493	281.24765	ESI-	-3.38	Oleic acid	C <sub>18</sub> H <sub>34</sub> O <sub>2</sub>	b,f,h,j	Organic acids
4	21.88	234.16135	233.15407	ESI-	-2.71	Eremophilenolide	C <sub>15</sub> H <sub>22</sub> O <sub>2</sub>	d	Esters
5	22.66	284.27035	283.26307	ESI-	-4.16	Stearic acid	C <sub>18</sub> H <sub>36</sub> O <sub>2</sub>	a,b,c,d,g,h,i,j	Organic acids
6	23.06	346.25027	345.24299	ESI-	-1.53	Troloxerutin	C <sub>22</sub> H <sub>34</sub> O <sub>3</sub>	h	Flavonoids
7	24.961	252.20838	251.20111	ESI-	-2.16	Hydrocarpic acid	C <sub>16</sub> H <sub>28</sub> O <sub>2</sub>	i	Organic acids
8	25.62	308.27129	307.26401	ESI-	-0.78	Mandenol	C <sub>20</sub> H <sub>36</sub> O <sub>2</sub>	b,j	Others
9	1.32	136.05231	137.05947	ESI+	-0.9	Phenylacetic acid	C <sub>8</sub> H <sub>8</sub> O <sub>2</sub>	h	Organic acids
10	6.175	204.08949	205.09677	ESI+	-1.9	D-Tryptophan	C <sub>11</sub> H <sub>12</sub> N <sub>2</sub> O <sub>2</sub>	h	Amino acids
11	6.642	354.09493	353.08766	ESI+	-0.42	Chlorogenic acid	C <sub>16</sub> H <sub>18</sub> O <sub>9</sub>	c	Phenylpropanoids
12	7.628	148.08861	149.09587	ESI+	-1.4	Cuminaldehyde	C <sub>10</sub> H <sub>12</sub> O	b,d,h	Aldehydes
13	7.922	228.07841	229.08569	ESI+	-1.02	Benzyl salicylate	C <sub>14</sub> H <sub>12</sub> O <sub>3</sub>	c	Esters
14	9.053	306.10998	307.11727	ESI+	-1.17	Cimifugin	C <sub>16</sub> H <sub>18</sub> O <sub>6</sub>	b	Coumarins
15	9.301	262.08375	261.07647	ESI+	-1.44	Vaginidiol	C <sub>14</sub> H <sub>14</sub> O <sub>5</sub>	g	Coumarins
16	10.904	260.10429	261.11156	ESI+	-2.2	Meranzin	C <sub>15</sub> H <sub>16</sub> O <sub>4</sub>	e	Phenylpropanoids
17	11.24	178.09901	179.1063	ESI+	-2.09	Methyl eugenol	C <sub>11</sub> H <sub>14</sub> O <sub>2</sub>	a,d,h,j	Phenylpropanoids
18	11.592	190.09891	191.1062	ESI+	-2.45	Ligustilide	C <sub>12</sub> H <sub>14</sub> O <sub>2</sub>	h,j	Phthalides
19	12.382	208.10921	207.10193	ESI+	-3.53	Elemicin	C <sub>12</sub> H <sub>16</sub> O <sub>3</sub>	a	Phenylpropanoids
20	12.63	226.11994	227.12723	ESI+	-2.52	Senkyunolide-N	C <sub>12</sub> H <sub>18</sub> O <sub>4</sub>	j	Phthalides
21	12.935	150.0678	151.07508	ESI+	-1.85	O-Acetyl-p-cresol	C <sub>9</sub> H <sub>10</sub> O <sub>2</sub>	d,j	Aromatic ketones
22	13.134	138.10423	139.11145	ESI+	-1.7	2-Pentylfuran	C <sub>9</sub> H <sub>14</sub> O	b,c,h,j,k	Others
23	13.6	210.12498	211.13227	ESI+	-2.91	Sedanoic acid	C <sub>12</sub> H <sub>18</sub> O <sub>3</sub>	j	Organic acids
24	14.257	270.05446	312.08832	ESI+	6.06	Apigenin	C <sub>15</sub> H <sub>10</sub> O <sub>5</sub>	a,j	Flavonoids
25	14.81	164.08336	165.09064	ESI+	-2.25	Eugenol	C <sub>10</sub> H <sub>12</sub> O <sub>2</sub>	h	Phenylpropanoids
26	15.112	192.04162	193.04899	ESI+	-3.31	Scopoletin	C <sub>10</sub> H <sub>8</sub> O <sub>4</sub>	b,c,d,g,h,k	Coumarins
27	15.21	162.03129	163.03857	ESI+	-2.49	Skimmetin	C <sub>9</sub> H <sub>6</sub> O <sub>3</sub>	c,d,g	Coumarins
28	15.462	302.07826	303.08533	ESI+	-2.58	Hesperetin	C <sub>16</sub> H <sub>14</sub> O <sub>6</sub>	e	Flavonoids
29	16.01	134.07293	135.08021	ESI+	-1.72	Apocynin	C <sub>9</sub> H <sub>10</sub> O	a,h	Aromatic ketones
30	16.348	188.08314	189.09042	ESI+	-3.12	3-Butylidene-phthalide	C <sub>12</sub> H <sub>12</sub> O <sub>2</sub>	h,j	Phthalides
31	16.995	234.16142	235.1687	ESI+	-2.38	Eremophilenolide	C <sub>15</sub> H <sub>22</sub> O <sub>2</sub>	d	Lignans
32	17.205	206.09356	251.09182	ESI+	-3.55	Senkyunolide-F	C <sub>12</sub> H <sub>14</sub> O <sub>3</sub>	j	Phthalides
33	17.776	255.25555	256.26283	ESI+	-2.61	Hexadecanamide	C <sub>16</sub> H <sub>33</sub> NO	h	Others
34	17.93	262.22902	280.26285	ESI+	-2.45	Farnesylacetone	C <sub>18</sub> H <sub>30</sub> O	h	Terpenoids
35	18.487	280.23949	281.24677	ESI+	-2.64	Linoleic acid	C <sub>18</sub> H <sub>32</sub> O <sub>2</sub>	b,h,j	Organic acids
36	18.75	196.14545	195.13817	ESI+	-4.48	Geranyl acetate	C <sub>12</sub> H <sub>20</sub> O <sub>2</sub>	b,h	Terpenoids
37	19.493	106.07842	107.0857	ESI+	1.6	O-xylene	C <sub>8</sub> H <sub>10</sub>	d,k	Others
38	19.608	194.13029	195.13757	ESI+	-2.01	Carvyl acetate	C <sub>12</sub> H <sub>18</sub> O <sub>2</sub>	a	Esters
39	19.95	264.20838	247.20507	ESI+	-2.07	Farnesol acetate	C <sub>17</sub> H <sub>28</sub> O <sub>2</sub>	a	Terpenoids
40	20.4	178.13538	179.14268	ESI+	-2.15	(2-Pentylphenyl) methanol	C <sub>12</sub> H <sub>18</sub> O	j	Others
41	20.8	128.08342	257.17413	ESI+	-2.38	Methyl 3-methyl-2-pentenoate	C <sub>7</sub> H <sub>12</sub> O <sub>2</sub>	i	Esters
42	21.552	142.13541	184.16913	ESI+	-2.47	Nonanal	C <sub>9</sub> H <sub>18</sub> O	b,d,h	Aldehydes
43	22.1	282.25466	281.24738	ESI+	-4.33	Oleic acid	C <sub>18</sub> H <sub>34</sub> O <sub>2</sub>	b,h,j	Organic acids
44	22.4	254.22391	255.23118	ESI+	-2.64	11-Hexadecenoic acid	C <sub>16</sub> H <sub>30</sub> O <sub>2</sub>	c	Organic acids
45	22.95	194.16667	177.16338	ESI+	-2.05	Geranyl acetone	C <sub>13</sub> H <sub>22</sub> O	b,h	Monoterpene ketones
46	23.27	256.23978	255.2325	ESI+	-1.74	Palmitic acid	C <sub>16</sub> H <sub>32</sub> O <sub>2</sub>	a,b,c,d,i,f,h,g,j	Organic acids
47	23.47	222.08875	205.08547	ESI+	-2.05	Monobutyl phthalate	C <sub>12</sub> H <sub>14</sub> O <sub>4</sub>	a	Esters
48	24.23	150.05303	149.04575	ESI+	1.35	DL-Arabinose	C <sub>5</sub> H <sub>10</sub> O <sub>5</sub>	h	Saccharides
49	25.2	284.27114	283.26386	ESI+	-1.38	Stearic acid	C <sub>18</sub> H <sub>36</sub> O <sub>2</sub>	a,b,c,d,i,h,g,j	Organic acids
50	25.416	252.20837	251.20109	ESI+	-2.21	Hydrocarpic acid	C <sub>16</sub> H <sub>28</sub> O <sub>2</sub>	i	Organic acids
51	26.1	308.27119	307.26391	ESI+	-1.12	Mandenol	C <sub>20</sub> H <sub>36</sub> O <sub>2</sub>	b,j	Esters
52	26.62	270.25547	269.2482	ESI+	-1.52	Heptadecanoic acid	C <sub>17</sub> H <sub>34</sub> O <sub>2</sub>	a,c	Organic acids

(Continued)

**Table I** (Continued).

No.	T <sub>R</sub> (min)	m/z		Ion Mode	ppm (10 <sup>-6</sup> )	Identification	Formula	Attribution	Classification
		Measured	Calculated						
53	26.81	144.04258	143.03515	ESI+	2.25	2,3-Dihydro-3,5-dihydroxy-6-methyl-4(H)-pyran-4-one	C <sub>6</sub> H <sub>8</sub> O <sub>4</sub>	k	Others
54	27.131	176.03243	175.02509	ESI+	1.93	Ascorbic Acid	C <sub>6</sub> H <sub>8</sub> O <sub>6</sub>	i	Others
55	27.234	118.02685	117.01946	ESI+	2.05	Succinic acid	C <sub>4</sub> H <sub>6</sub> O <sub>4</sub>	a	Organic acids
56	27.47	118.02685	117.01946	ESI+	2.05	p-coumaric acid	C <sub>9</sub> H <sub>8</sub> O <sub>3</sub>	a,c	Phenylpropanoids

Notes: a. Jing-Jie, b. Fang-Feng, c. Qiang-Huo, d. Du-Huo, e. Zhi-Ke, f. Fu-Ling, g. Qian-Hu, h. Chai-Hu, i. Jie-Geng, j. Chuang-Xiong, k. Gan-Cao.

## Molecular Docking Probes the Binding Ability of Phytochemicals of JFG in Serum to Target Proteins

To further identify the targets of the phytochemicals of JFG in serum, molecular docking was performed between the individual phytochemicals of JFG in serum and candidate target proteins with higher degrees in the PPI network and

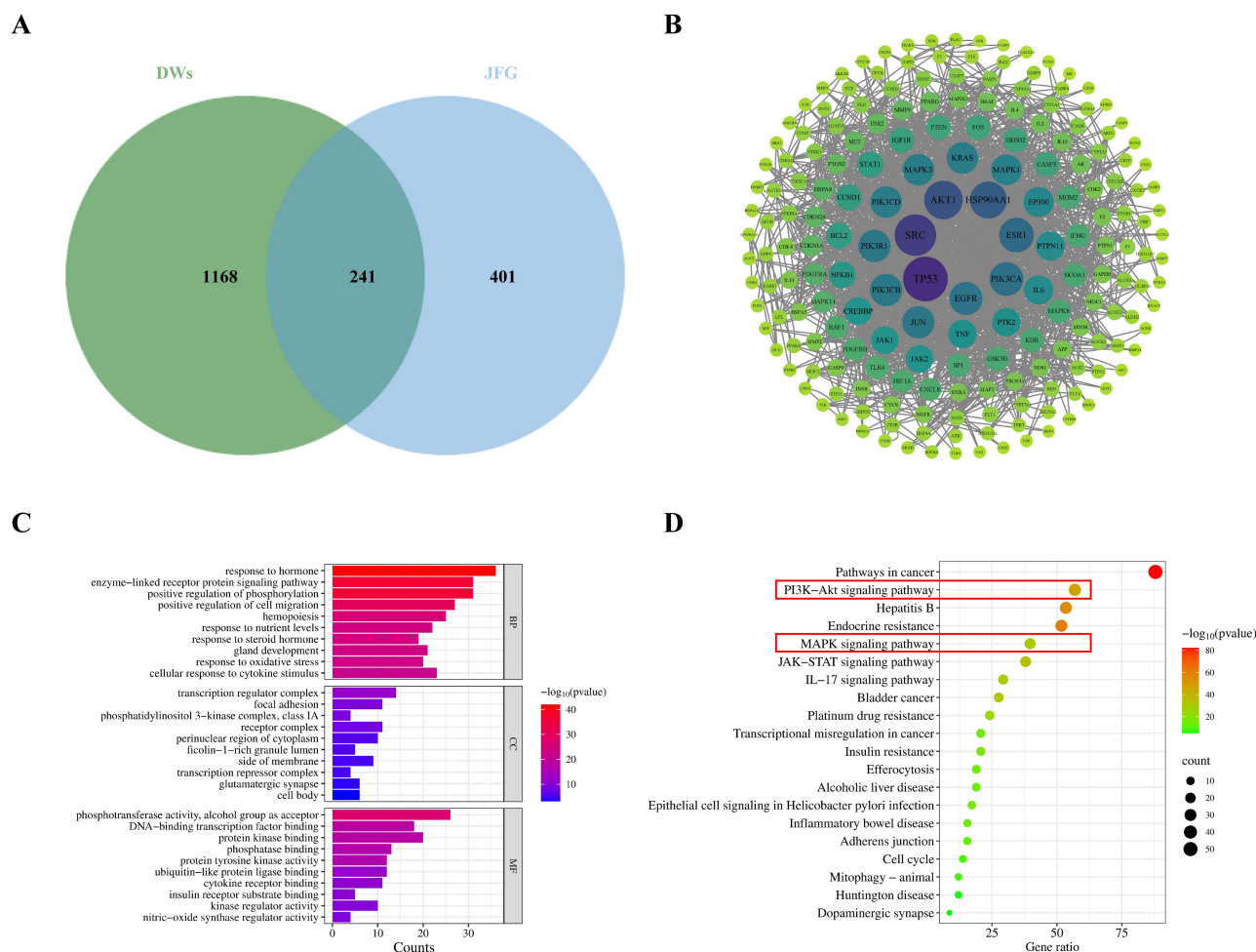


**Figure 7** Network pharmacological analysis of phytochemicals of JFG in serum in diabetic wounds therapy. **(A)** Venn diagram of common targets of diabetic wounds and phytochemicals of JFG in serum. **(B)** The confidence interval was set to “Highest” (≥ 0.9), and the disconnected nodes were hide to construct the PPI network, which was input into Cytoscape 3.8.0 for visual analysis to acquire the core targets of phytochemicals of JFG in serum against diabetic wounds. Nodes served as the potential targets, and the size and color depth of the nodes corresponded positively to the degree value. The gray edges represented the interaction among the targets. **(C)** Gene Ontology enrichment analysis. **(D)** Kyoto Encyclopedia of Genes and Genomes pathway enrichment analysis.

other targets closely associated with diabetic wounds. The 6 selected candidate target proteins, AKT1, EGFR, MAPK3, MAPK1, IL6, and TNF, were subjected to docking with 49 non-repetitive phytochemicals of JFG in the serum. The docking results showed that most of the phytochemicals had good binding ability to candidate target proteins, with a binding energy of less than  $-5.0$  kcal/mol (Figure 8A).

The interactions between the highest-affinity phytochemical and the protein are shown in Figure 8B–G. Eremophilenolide mainly forms 1 hydrogen bond with residue LYS39 on AKT1 protein. Hesperetin mainly forms 2 hydrogen bonds with residues LEU788 and THR790 on the EGFR protein and 4 hydrogen bonds with residues MET108, GLN105, SER153, and ASP111 on the MAPK1 protein. Apigenin mainly forms 2 hydrogen bonds with residues GLY148 and PHE144 on the TNF protein, forming 2 hydrogen bonds with residues ARG30 and GLN175 on the IL6 protein, and 4 hydrogen bonds with residues ALA188, GLN83, ARG83 and THR80 on the MAPK3 protein. Collectively, molecular docking results predicted that most phytochemicals of JFG in the serum could bind well to 6 core targets of diabetic wounds (AKT1, EGFR, MAPK3, MAPK1, IL6, and TNF), all of which might play key roles in improving diabetic wounds.

## JFG Regulates PI3K-AKT and MAPK Signaling Pathways to Promote Diabetic Wound Healing in Diabetic Rats

Considering that we enriched the PI3K-AKT and MAPK signaling pathways in the KEGG analysis (Figure 7B–D) as the molecular mechanism of JFG phytochemicals in serum for the enhancement of diabetic wounds, we further validated the PI3K-AKT and MAPK signaling pathways in the wound tissues of diabetic rats by Western blotting. The suppression of the PI3K-AKT signaling pathway is not only implicated in hyperglycemia-induced metabolic dysregulation but also critically contributes to the delayed healing of diabetic wounds.<sup>10</sup> The hyperglycemic state of diabetic patients activates the MAPK signaling pathway, and the overexpression of MAPK promotes the development of diabetic wounds while blocking the MAPK pathway may play a therapeutic role.<sup>34</sup> In comparison with the control group, the phosphorylation of AKT in wound tissue was significantly reduced in the model group which could be reversed by JFG in diabetic rats (Figure 9A and B, Model group vs Control group,  $p < 0.05$ ; JFG-1 g/kg vs Model group,  $p > 0.05$ ; JFG-2 g/kg vs Model group,  $p < 0.05$ ). As shown in Figure 9C–H, the phosphorylation of ERK, P38, and JNK, which was upregulated in the model group compared to the control group (Model group vs Control group,  $p < 0.01$ ), was significantly restored by JFG (p-ERK, p-P38, p-JNK: JFG-1 g/kg vs Model group,  $p < 0.01$ ; JFG-2 g/kg vs Model group,  $p < 0.01$ ), demonstrating that JFG could inhibit the MAPK signaling pathway in STZ-induced diabetic rats. Taken together, these results suggest that activation of the PI3K-AKT signaling pathway and inhibition of the MAPK signaling pathway are involved in JFG's promotion of wound healing in diabetic rats.

## Discussion

Diabetic wounds are chronic refractory wounds caused by multiple factors such as hyperglycemia, inflammation, oxidative stress and tissue hypoxia/impaired vascular adaptation.<sup>7</sup> Additionally, hyperglycemia-induced immune dysregulation and microvascular leakage result in an alkaline shift in wound pH,<sup>35</sup> an elevated bacterial burden,<sup>36</sup> and subsequent infection.<sup>37</sup> This cascade perpetuates prolonged inflammation, ultimately leading to delayed and impaired wound repair. It is the complexity of diabetic wounds pathogenesis that makes it difficult to treat diabetic wounds by targeting a single mechanism. Characterized by its multi-target, multi-approach, and multi-level pharmacological activities, traditional Chinese medicine is widely considered suitable for the treatment of diabetic wounds.<sup>10</sup> JFG, a traditional Chinese medicine derived from the classic formula Jingfang Baidu Powder, has been widely used for the treatment of cold caused by wind and cold in China and our previous studies have evaluated its toxicity profile and safety both in animal models and clinical application.<sup>11,38,39</sup> Previous studies have demonstrated that JFG possesses potent anti-inflammatory and antioxidant activities, contributing to the alleviation of various skin diseases including acne,<sup>19</sup> psoriasis,<sup>20</sup> urticaria,<sup>21</sup> etc. Additionally, JFG demonstrates significant antibacterial efficacy, exhibiting therapeutic potential against pneumonia induced by *Pseudomonas aeruginosa* and *Staphylococcus aureus*.<sup>11,40</sup> Thus, we speculate that JFG has potential for the treatment of diabetic wounds. In this study, we demonstrated that JFG promoted

A

Vaginalinal	-6.084	-8.620	-6.119	-6.313	-7.754	-7.219
Palmitic acid	-3.951	-6.661	-4.182	-4.021	-4.578	-4.114
Oleic acid	-4.153	-6.920	-4.116	-4.546	-5.257	-4.444
Eremophilinolide	-7.084	-7.878	-6.413	-6.175	-7.138	-7.077
Stearic acid	-5.727	-6.828	-4.721	-4.955	-4.890	-4.801
Troscerutin	-6.505	-9.205	-6.897	-6.217	-8.060	-7.075
Hydrocarpic acid	-4.261	-7.418	-4.772	-4.491	-5.545	-5.285
Mandelol	-4.198	-7.075	-4.129	-3.823	-4.951	-4.918
Phenylacetic acid	-4.966	-6.263	-5.791	-5.496	-6.628	-5.293
D-Tryptophan	-5.878	-7.491	-5.487	-5.837	-6.416	-6.336
Chlorogenic acid	-6.311	-8.520	-6.227	-6.578	-7.667	-7.308
Cuminaldehyde	-5.647	-6.461	-5.417	-4.928	-5.711	-5.281
Benzyl salicylate	-6.120	-8.790	-5.557	-6.019	-6.657	-6.265
Cimifugin	-6.047	-4.807	-6.556	-6.235	-7.514	-6.771
Meranzin	-5.672	-8.208	-6.254	-6.049	-7.528	-6.948
Methyl Eugenol	-4.282	-7.004	-4.741	-5.086	-5.703	-5.666
Ligustilide	-5.218	-7.518	-5.550	-5.720	-6.341	-5.947
Elemicin	-4.622	-6.010	-5.246	-4.790	-5.873	-5.296
Senkuniolide-N	-5.442	-7.898	-5.667	-5.645	-6.419	-6.088
O-Acetyl-p-cresol	-5.293	-6.661	-5.794	-5.099	-5.873	-5.684
2-Pentylfuran	-4.299	-5.808	-4.262	-3.897	-4.543	-4.278
Secalonic acid	-5.442	-7.488	-5.413	-5.452	-6.361	-5.807
Apigenin	-6.324	-8.704	-7.030	-6.833	-8.724	-7.510
Eugenol	-4.917	-6.407	-5.221	-5.135	-5.751	-5.360
Scopoletin	-5.329	-7.152	-5.326	-5.582	-6.693	-6.108
Skimmetin	-5.425	-7.072	-6.674	-5.646	-6.348	-6.193
Hesperetin	-6.179	-8.566	-6.899	-6.085	-8.240	-7.559
Apocynin	-4.875	-4.235	-5.649	-5.198	-5.685	-5.267
3-Benzyldeneephthalide	-5.285	-7.685	-5.372	-5.184	-6.534	-6.063
Senkuniolide-F	-5.264	-7.797	-5.685	-5.424	-6.689	-6.383
Hexadecanamide	-4.356	-6.685	-3.915	-4.418	-4.689	-4.605
Farnesylacetone	-5.382	-8.216	-4.874	-5.433	-5.980	-5.474
Linoleic acid	-3.298	-7.232	-4.608	-5.086	-5.644	-4.991
Geranyl acetate	-4.325	-7.029	-5.272	-5.167	-5.561	-5.090
Oxylene	-4.542	-5.432	-4.473	-4.364	-5.043	-4.760
Carvyl acetate	-5.154	-7.825	-5.714	-5.292	-6.100	-5.970
Farnesol acetate	-4.867	-8.333	-4.836	-4.895	-6.054	-5.327
(2-Pentylphenyl)methanol	-4.827	-6.997	-5.345	-5.089	-5.837	-5.447
Methyl 3-methyl-2-pentenoate	-4.330	-5.236	-4.162	-4.207	-4.768	-4.352
Nonanal	-3.697	-5.445	-3.976	-3.728	-4.479	-4.084
11-Hexadecenoic acid	-5.249	-4.664	-4.849	-4.076	-4.502	-4.882
Geranylacetone	-5.664	-7.374	-5.289	-5.081	-5.421	-5.172
Monobutyl phthalate	-4.765	-6.704	-4.945	-5.228	-5.841	-5.781
DL-Arabinose	-4.471	-4.959	-4.184	-4.027	-5.227	-4.490
Heptadecanoic acid	-4.182	-6.468	-3.844	-4.392	-4.787	-4.654
2,3-Dihydro-3,5-dihydroxy-6-methyl-4(H)-pyran-4-one	-4.889	-6.091	-5.122	-4.668	-5.258	-4.814
Ascorbic acid	-4.975	-5.876	-5.376	-5.097	-6.407	-5.281
Succinic acid	-4.446	-5.202	-4.796	-4.322	-4.695	-4.230
p-coumaric acid	-5.324	-7.169	-5.968	-5.489	-5.958	-5.663

Affinity (kcal/mol)

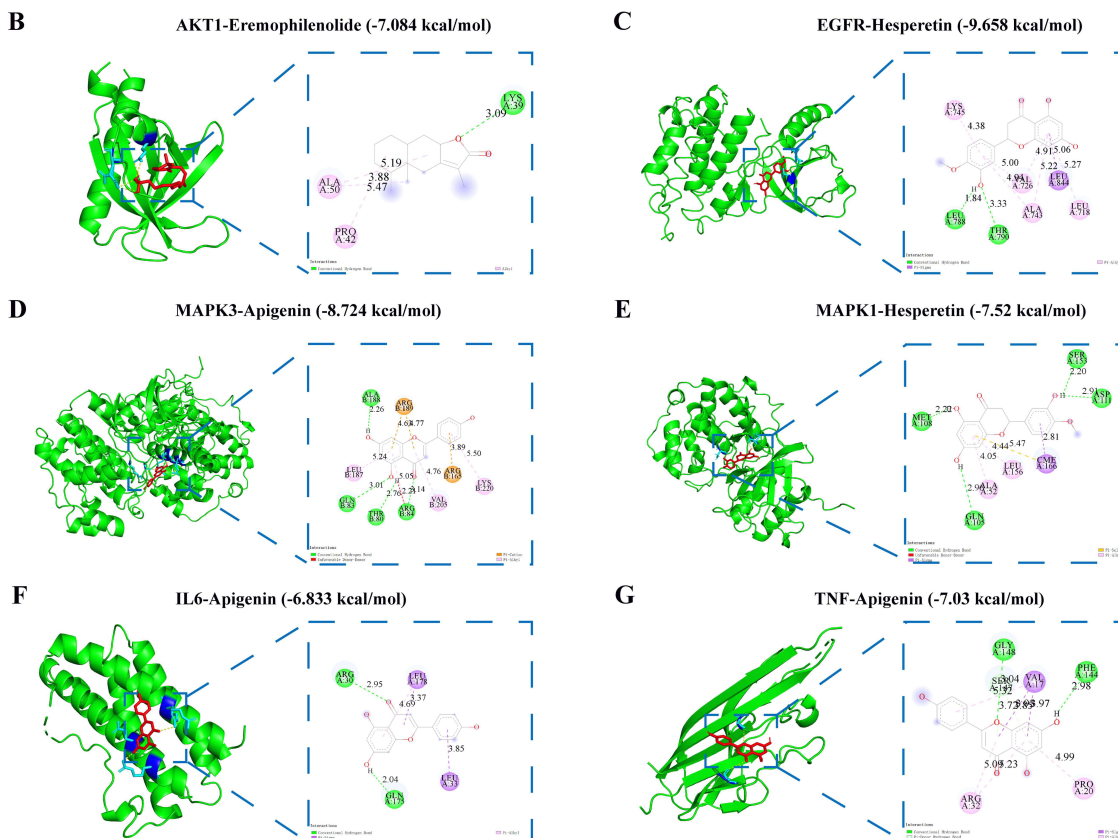


**Figure 8** Molecular docking diagram of targets and their strongest binding phytochemicals of JFG in serum. **(A)** Lowest binding energy for the ligand-protein interactions detected by molecular docking. **(B)** The 3D and 2D diagrams of AKTI and Eremophilinolide. **(C)** The 3D and 2D diagrams of EGFR and Hesperetin. **(D)** The 3D and 2D diagrams of MAPK3 and Apigenin. **(E)** The 3D and 2D diagrams of MAPK1 and Hesperetin. **(F)** The 3D and 2D diagrams of IL6 and Apigenin. **(G)** The 3D and 2D diagrams of TNF and Apigenin.

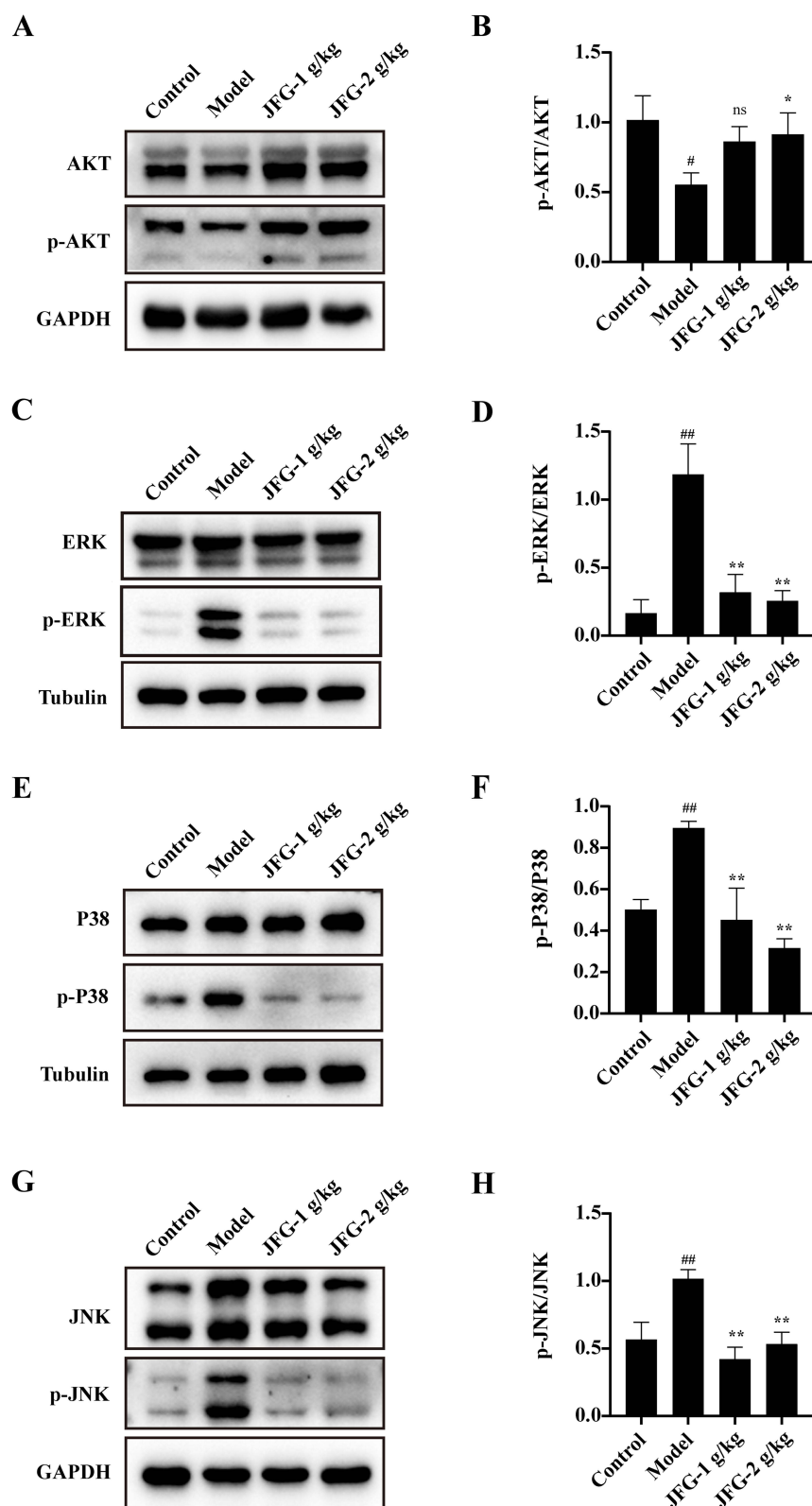


**Figure 9** JFG regulates PI3K-AKT and MAPK signaling pathways in the wound tissues of diabetic rats. Rats pre-administered orally with JFG were induced diabetes by streptozotocin and wounds were made, followed by continued administration until day 23, then the wound tissues were harvested and proteins were extracted. **(A and B)** Western blot analysis of Protein Kinase B (AKT) and phosphorylated AKT (P-AKT). **(C and D)** Western blot analysis of Extracellular Signal-Regulated Kinase (ERK) and phosphorylated ERK (p-ERK). **(E and F)** Western blot analysis of p38 Mitogen-Activated Protein Kinase (P38) and phosphorylated p38 Mitogen-Activated Protein Kinase (p-P38). **(G and H)** Western blot analysis of c-Jun N-terminal Kinase (JNK) and phosphorylated JNK (p-JNK). Data are expressed as mean  $\pm$  SD of independent experiments. # $p < 0.05$ , ## $p < 0.01$  vs control group; \* $p < 0.05$ , \*\* $p < 0.01$  vs model group; "ns" indicates "not significant" ( $p > 0.05$ ).

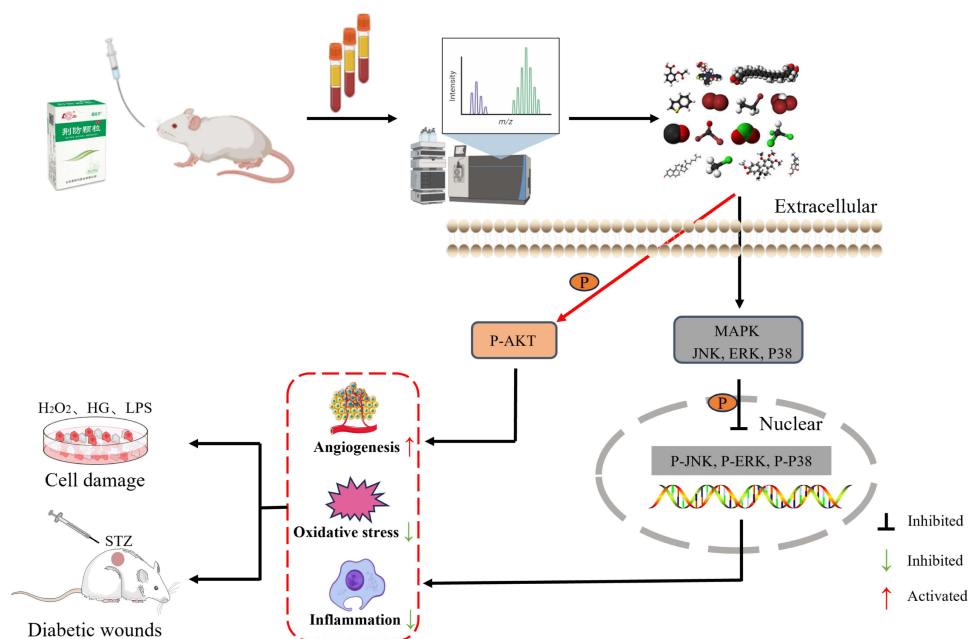


**Figure 10** Potential mechanisms of JFG for the treatment of diabetic wounds.

angiogenesis, ameliorated excessive oxidative stress, alleviated inflammation response and regulated metabolic abnormalities, which ultimately promoted diabetic wound healing (Figure 10). Our results provided compelling evidence that JFG is a promising treatment option for diabetic wounds. Simultaneously, our findings also reveal the promising potential of traditional Chinese medicine to treat diabetic wounds.

Excessive oxidative stress directly delays diabetic wound healing by impairing endothelium-mediated vascular homeostasis.<sup>41</sup> The hyperglycemic state impairs re-epithelialization of keratinocytes and thus impedes diabetic wound healing.<sup>42</sup> It has been reported that total iridoid glycoside extract of *L. rotata* raised plasma levels of SOD and CAT while lowering the levels of ROS and MDA thereby accelerating wound healing in db/db mice.<sup>43</sup> Our results indicated that JFG could exert cytoprotective effects on both H<sub>2</sub>O<sub>2</sub>-induced and HG-induced damage in HUVECs and HaCaT cells (Figure 1C–F). In addition, we found that JFG treatment significantly alleviated oxidative stress in diabetic rats, as evidenced by the upregulation of SOD and downregulation of MDA, MPO, and GSSG (Figure 5E–H). The excellent antioxidative stress effects of JFG have also been demonstrated in other diseases. For example, JFG significantly reduced the levels of ROS and MDA, while significantly increased the levels of SOD, CAT and GSH in myocardial tissues of rats with acute myocardial infarction.<sup>16</sup> Taken together, our findings suggest that alleviating oxidative stress is one of the mechanisms by which JFG intervenes in diabetic wounds and other oxidative stress related diseases.

Inflammation is the first stage of normal wound healing, followed by proliferation and remodeling. In this phase, monocytes differentiate into M1 macrophages, which release extensive pro-inflammatory cytokines and play a critical role in the removal of pathogen and cell debris.<sup>44,45</sup> In diabetic wounds, the wound is stalled in a persistent inflammatory phase, ultimately resulting in delayed healing.<sup>44,46</sup> The current study revealed the anti-inflammatory effect of JFG in both the LPS-simulated RAW264.7 cell model and the wound tissues of diabetic rats presented by downregulated pro-inflammatory cytokines including IL-6, TNF- $\alpha$  and IL-1 $\beta$  (Figures 2A, B and 5I–K), which was consistent with previous studies of JFG in other inflammatory pathological states such as acute lung, urticaria, *Pseudomonas aeruginosa* pneumonia and psoriasis.<sup>11,20,21,27</sup> From a mechanistic perspective, abnormal activation of the MAPK-NF $\kappa$ B signaling pathway is an important mechanism leading to persistent inflammatory response in diabetic wounds.<sup>47</sup> SCIO-469, a selective p38 $\alpha$  inhibitor, improved impaired wound healing in db/db mice;<sup>48</sup> Qizhi Jiangtang Capsule (QJC), contributes to the healing of skin wounds and reduction of inflammation in diabetic rats by inhibiting the phosphorylation of ERK.<sup>49</sup> JFG has been shown to alleviate various inflammatory diseases by modulating the MAPK signaling pathway. These results were consistent with our finding that JFG alleviated inflammation and accelerated wound healing in

diabetic rats by inhibiting the MAPK signaling pathway (Figure 9C–H). However, it is critical to highlight that while JFG addresses both diabetic wounds and other inflammatory diseases through the same mechanism targeting the MAPK signaling pathway, our present study uniquely investigates the efficacy of JFG on skin ulcers under metabolic stress conditions, a scenario rarely explored before. Furthermore, JFG has been reported to suppress glycolysis, the predominant metabolic pathway providing rapid energy for activated immune cells, thereby alleviating inflammation in OVA/aluminum hydroxide-induced urticaria in vivo.<sup>21</sup> Activated macrophages, commonly classified as the classically activated (M1) subtype, demonstrate a pronounced upregulation of glycolytic flux. This metabolic reprogramming serves as a critical metabolic prerequisite for the acquisition of their pro-inflammatory effector functions, including the synthesis and secretion of cytokines such as TNF- $\alpha$  and IL-6.<sup>50</sup> However, in our present study, JFG inhibited the expression of pro-inflammatory cytokines without suppressing glycolysis in LPS induced RAW264.7 cells under the present experimental conditions (Figure 2C and D), suggesting a potential decoupling between glycolytic metabolism and inflammatory responses. This decoupling between glycolytic metabolism and inflammatory responses were also observed in other studies. For example, TGF- $\beta$  enhances glycolysis via the mTOR-c-MYC pathway, additionally, it reduces pro-inflammatory cytokine production through the suppression of inflammatory transcription factors and activation of SMAD3.<sup>50</sup> Furthermore, trained macrophages (exposed to LPS derivatives and other PAMPs) demonstrate heightened glycolysis and reduced inflammatory cytokine production, conferring protective effects in infection models.<sup>51</sup> Thus, other mechanisms rather than metabolic rearrangement may mediate the anti-inflammatory activity of JFG serum during LPS-stimulated inflammation.

Angiogenesis, involving the proliferation, migration, and tube formation of endothelial cells, is an essential process in wound healing.<sup>29</sup> Isolated from *Panax notoginseng* leaves, notoginsenoside Ft1 accelerated diabetic wound healing by promoting the formation of new blood vessels and increasing VEGF, PDGF and FGF levels around the wounds.<sup>52</sup> Our results showed that JFG significantly elevated the migratory and angiogenic capacities of HUVECs (Figure 3). Similarly, in vivo, JFG treatment significantly increased the proportion of CD31-positive endothelial cells compared to that in the untreated model group (Figure 4G–H), implying that JFG indeed contributes to neovascularization in the skin wound tissue of diabetic rats. It has been reported that the inhibited HIF-1 $\alpha$ -VEGF and PI3K-AKT signaling pathways are related to diabetic angiogenesis disorders, and that repair of these two pathways could effectively promote angiogenesis in diabetic wounds.<sup>10,53</sup> Since JFG markedly restored AKT phosphorylation in the wound tissues of diabetic rats (Figure 9A and B), it is reasonable to speculate that JFG promotes angiogenesis by reversing the suppressed PI3K-AKT signaling pathway. However, other possible mechanisms maybe also involved and will be investigated further in subsequent studies.

In addition to the systemic hyperglycemic state, diabetes also induces other metabolic disorders such as dyslipidemia, leading to delayed wound healing. JFG has been reported to improve glucose and lipids metabolism disturbance in several disease states, for instance, reducing blood glucose thereby increasing body weight and ameliorating retinopathy in db/db mice.<sup>32</sup> Similarly, in our study, JFG notably decreased the level of glucose, TG and T-CHO in blood (Figure 5B–D), further alleviating weight loss (Figure 5A) as well as promoting wound healing in diabetic rats. Our findings are in line with other investigations showing that *Polygonatum kingianum* Collett & Hemsl promoted wound healing by reducing blood glucose levels in STZ-induced diabetic rats.<sup>54</sup> The PI3K-AKT signaling pathway, which is critically associated with glucose metabolism, plays an essential regulatory role in the pathophysiological mechanisms underlying diabetic wound healing.<sup>10</sup> Naoxintong capsule (NXT), a prescribed traditional Chinese medicine,<sup>55</sup> promoted diabetic wound healing by enhancing angiogenesis and collagen deposition via the activation of the PI3K-AKT signaling pathway. Consistently, we found that JFG effectively reversed the inactivated PI3K-AKT signaling pathway in diabetic wounds, which may contribute to the regulation of glucose and lipid metabolism (Figure 5B–D) as well as the promotion of collagen enrichment in wound tissues (Figure 4E and F). Therefore, based on our present work and previous studies, in addition to regulating oxidative stress, inflammation, and angiogenesis, modulating blood glucose and lipid metabolism is equally important for promoting diabetic wound healing. Traditional Chinese medicine, represented by JFG, possesses the multiple functions mentioned above, and effectively fulfills the treatment needs of diabetic wounds.

Comprising 11 herbal components, JFG includes hypoglycemic agents (*Saposhnikovia divaricata* (Turcz. ex Ledeb.) Schischk. (Fang Feng), *Conioselinum anthriscoides* (Chuan Xiong), *Poria cocos* (Schw.) Wolf (Fu Ling)),<sup>32</sup> anti-

inflammatory constituents (*Nepeta cataria* L. (Jing Jie), *Hansenia weberbaueriana* (Fedde ex H. Wolff) Pimenov & Kljuykov (Qiang Huo), and *Glycyrrhiza uralensis* Fisch. ex DC. (Gan Cao)),<sup>56–58</sup> and antioxidants (*Heracleum hemsleyanum* Diels (Du Huo), *Bupleurum chinense* DC. (Chai Hu), and *Citrus aurantium* L. (Zhi Qiao)).<sup>59–61</sup> Its active compounds synergistically target diabetic wound pathology, characterized by chronic inflammation, oxidative stress, and metabolic dysregulation, through multi-mechanistic actions, exemplifying the polypharmacological advantages of traditional Chinese medicine in managing multifactorial diseases. The phytochemicals of JFG (including scopoletin, troxerutin, hesperetin, etc.) have been well defined and widely reported in our previous study.<sup>12–14</sup> In our present study, as shown in Figure 6 and Table 1, 56 serum prototypes of JFG were analyzed and identified. Among them, some show clear or strong potential to improve diabetic wound healing. Chlorogenic acid,<sup>62</sup> apigenin,<sup>63</sup> eugenol,<sup>64</sup> and ascorbic acid<sup>65</sup> work by reducing inflammation, fighting oxidative stress, and aiding tissue repair. Other compounds like troxerutin<sup>13</sup> and hesperetin<sup>14</sup> might also promote healing due to their anti-inflammatory, antioxidant, and blood vessel-protecting properties. All of these phytochemicals aforementioned may play an indispensable role in JFG-mediated promotion of diabetic wound healing.

Our previous studies have shown that JFG is able to treat other diseases such as lung inflammation and urticaria. The major novelty of our present work is the identification of a novel indication for JFG, along with its mechanisms, partly by regulating the PI3K-AKT and MAPK signaling pathways. Although PI3K-AKT and MAPK signaling pathways are common signaling pathways, it was previously unclear whether regulation of the PI3K-AKT and MAPK signaling pathways could promote healing of diabetic wounds in the presence of JFG, which our study illustrated for the first time. Nonetheless, certain limitations remain in the present study and require refinement in future investigations. For example, our previous study demonstrated that JFG exhibits potent therapeutic efficacy against *Pseudomonas aeruginosa*-induced and *Staphylococcus aureus*-induced murine pneumonia.<sup>11,40</sup> However, in this work, we focused exclusively on sterile wound healing-associated inflammation induced by hyperglycemia alone, subsequent investigations will prioritize evaluating JFG's immunomodulatory effects on bacterial infection-induced inflammation. Another issue that should be noted is that current pharmacodynamic studies of diabetic wounds lack a standardized therapeutic reference. Since ON101 have been approved by China's NMPA in November 2023 to treat diabetic foot ulcers, ON101 in the near future could be considered as a potential reference control in subsequent experimental designs. Additionally, in this present work, only a 14-day post-wounding observation was conducted on the initial healing cascade; our future studies will extend this observation to 28 days post-injury to evaluate JFG's impact on both initial healing and late-stage healing outcomes. Though this study has already validated several high-priority targets, future work should systematically test additional candidates (eg, BCL2, NFKB1) using multi-omics approaches, conduct external validation of the findings and further confirm the binding of the serum phytochemicals to these identified target proteins.

One common problem in traditional Chinese medicine research is the complexity of its pharmacokinetic studies. Currently absorption, distribution, metabolism, and excretion (ADME) pharmacokinetic and bioavailability studies of traditional Chinese medicine formulas are hindered by inherent complexities, including undefined active constituents and methodological constraints in component analysis. Thus, these challenges have precluded characterization of JFG's pharmacokinetic profile. Future advancements in analytical technologies and the elucidation of pivotal bioactive constituents are expected to resolve these problems. Therefore, in our future research work, bioavailability and ADME pharmacokinetics of JFG will be explored sooner or later. Nevertheless, in our present work, the preclinical efficacy of JFG in promoting diabetic wound healing has been well-established, demonstrating considerable potential for clinical translation in managing diabetic foot ulcer patients, and subsequent clinical development will be conducted for the treatment of diabetic wounds.

## Conclusion

In summary, our study demonstrated that JFG alleviated oxidative damage, promoted angiogenesis, and suppressed inflammation in vitro. In STZ-induced diabetic rats, JFG effectively accelerated diabetic wound healing by promoting angiogenesis, regulating metabolic abnormalities, and alleviating inflammation and oxidative stress. A total of 56 serum phytochemicals of JFG were identified, and most of the phytochemicals absorbed in the serum docked well to the key diabetic wounds related targets (AKT1, EGFR, MAPK3, MAPK1, IL6, and TNF). Restoration of the PI3K-AKT and MAPK signaling pathways is a key mechanism mediating the therapeutic effect of JFG on diabetic wounds. We found for

the first time that JFG has potential for the treatment of diabetic wounds by alleviating oxidative stress, suppressing inflammatory responses, and promoting angiogenesis, providing a new perspective on the novel application of JFG and demonstrating considerable potential for clinical translation in managing diabetic foot ulcer patients.

## Abbreviations

JFG, Jingfang Granules; HG, high glucose; OD, optical density; STZ, streptozotocin; i.g., intragastrical administration; CD31, platelet endothelial cell adhesion molecule-1; TG, triglyceride; T-CHO, total cholesterol; SOD, superoxide dismutase; MDA, malondialdehyde; MPO, myeloperoxidase; GSSG, glutathione oxidized; ESI, electrospray ionization; PPI, protein-protein interaction; GO, Gene Ontology; KEGG, Kyoto Encyclopedia of Genes and Genomes; BP, Biological Process; CC, Cellular Component; MF, Molecular Function; ROS, reactive oxygen species.

## Ethics Approval and Informed Consent

This study was approved by the Institutional Animal Care and Use Committee of the Ocean University of China (OUC-SMP-2023-12-02).

## Acknowledgment

We thank BioRender (Created in BioRender. Wang, Q. (2025) <https://BioRender.com/q1qehok>) and bioicons (<https://bioicons.com/>, macrophage icon by Servier <https://smart.servier.com/> is licensed under CC-BY 3.0 Unported <https://creativecommons.org/licenses/by/3.0/>, angiogenesis icon by Servier <https://smart.servier.com/> is licensed under CC-BY 3.0 Unported <https://creativecommons.org/licenses/by/3.0/>, western blotting icon by Pooja is licensed under CC-BY 4.0 Unported <https://creativecommons.org/licenses/by/4.0/>, gel-electrophoresis icon by Servier <https://smart.servier.com/> is licensed under CC-BY 3.0 Unported <https://creativecommons.org/licenses/by/3.0/>, rat-adult icon by Servier <https://smart.servier.com/> is licensed under CC-BY 3.0 Unported <https://creativecommons.org/licenses/by/3.0/>, 96\_well\_plate icon by Marcel Tisch <https://twitter.com/MarcelTisch> is licensed under CC0 <https://creativecommons.org/publicdomain/zero/1.0/>, 24-well-plate icon by Servier <https://smart.servier.com/> is licensed under CC-BY 3.0 Unported <https://creativecommons.org/licenses/by/3.0/>, tube-rack icon by DBCLS <https://togotv.dbcls.jp/en/pics.html> is licensed under CC-BY 4.0 Unported <https://creativecommons.org/licenses/by/4.0/>, wound-healing icon by Servier <https://smart.servier.com/> is licensed under CC-BY 3.0 Unported <https://creativecommons.org/licenses/by/3.0/>) for providing access to scientific illustration tools essential for this study. We thank Dr. Lu for granting permission to use the cell damage images from their 2022 study (Lu X, Liu M, Dong H, Miao J, Stagos D, Liu M. Dietary prenylated flavonoid xanthohumol alleviates oxidative damage and accelerates diabetic wound healing via Nrf2 activation. *Food Chem Toxicol.* Feb 2022;160:112813. doi:10.1016/j.fct.2022.112813). We also thank Dr Stagos Dimitrios, university of Thessaly in Greece, for his editing and suggestions on the language of the manuscript.

## Author Contributions

All authors made significant contributions to the work reported, whether in conceptualization, research design, execution, data acquisition, analysis, and interpretation or in all of these areas. They also participated in the drafting, revision, or critical review of the manuscript as well as the final approval of the version to be published. They reached a consensus on the submission of the article to the journal and agreed to be responsible for all the aspects of this study.

## Funding

This research was supported by the Special Fund for Local Science and Technology Development Guided by the Central Government (YDZX2023014), Natural Science Foundation of Shandong Province (ZR2024MH291), Qingdao Science and Technology Benefiting the People Demonstration Special Project (24-1-8-smjk-19-nsh), and Key Technology Research and Industrialization Demonstration Projects in Qingdao (23-1-4-xxgg-13-nsh, 24-1-4-xxgg-17-nsh). This research was also supported by Key R&D Program of Shandong Province, China (2021CXGC010508) and project Joint Foundation for Innovation and Development supported by Shandong Provincial Natural Science Foundation (ZR2022LZY021).

## Disclosure

The authors declare no conflict of interest.

## References

- Boulton AJM. The diabetic foot: grand overview, epidemiology and pathogenesis. *Diabetes Metab Res Rev.* 2008;24(1):S3–S6. doi:10.1002/dmrr.833
- Kandhare AD, Ghosh P, Bodhankar SL. Naringin, a flavanone glycoside, promotes angiogenesis and inhibits endothelial apoptosis through modulation of inflammatory and growth factor expression in diabetic foot ulcer in rats. *Chem Biol Interact.* 2014;219:101–112. doi:10.1016/j.cbi.2014.05.012
- Lin SY, Zhang Q, Li SH, et al. Antioxidative and angiogenesis-promoting effects of tetrahedral framework nucleic acids in diabetic wound healing with activation of the Akt/Nrf2/HO-1 pathway. *ACS Appl Mater Interfaces.* 2020;12(10):11397–11408. doi:10.1021/acsami.0c00874
- Hart CE, Loewen-Rodriguez A, Lessem J. Dermagraft: use in the treatment of chronic wounds. *Adv Wound Care.* 2012;1(3):138–141. doi:10.1089/wound.2011.0282
- Dinh TL, Veves A. The efficacy of apligraf in the treatment of diabetic foot ulcers. *Plast Reconstr Surg.* 2006;117(7):152S–157S. doi:10.1097/01.prs.0000222534.79915.d3
- Hicks CW, Zhang GQ, Canner JK, et al. Outcomes and predictors of wound healing among patients with complex diabetic foot wounds treated with a dermal regeneration template (integra). *Plast Reconstr Surg.* 2020;146(4):893–902. doi:10.1097/PRS.00000000000007166
- Matoori S, Veves A, Mooney DJ. Advanced bandages for diabetic wound healing. *Sci Transl Med.* 2021;13(585). doi:10.1126/scitranslmed.abe4839
- Wang F, Zhang X, Zhang J, et al. Recent advances in the adjunctive management of diabetic foot ulcer: focus on noninvasive technologies. *Med Res Rev.* 2024;44(4):1501–1544. doi:10.1002/med.22020
- Lin CW, Chen CC, Huang WY, et al. Restoring prohealing/remodeling-associated M2a/c macrophages using ON101 accelerates diabetic wound healing. *JID Innov.* 2022;2(5):100138. doi:10.1016/j.xjidi.2022.100138
- Zhou X, Guo Y, Yang K, Liu P, Wang J. The signaling pathways of traditional Chinese medicine in promoting diabetic wound healing. *J Ethnopharmacol.* 2022;282:114662. doi:10.1016/j.jep.2021.114662
- Gu MD, Su W, Dai JQ, et al. Jingfang granule alleviates *Pseudomonas aeruginosa*-induced acute lung inflammation through suppression of STAT3/IL-17/NF- $\kappa$ B pathway based on network pharmacology analysis and experimental validation. *J Ethnopharmacol.* 2023;318(Pt A):116899. doi:10.1016/j.jep.2023.116899
- Zhang J, Yuan Y, Gao X, et al. Scopoletin ameliorates hyperlipidemia and hepatic steatosis via AMPK, Nrf2/HO-1 and NF- $\kappa$ B signaling pathways. *Biochem Pharmacol.* 2025;231:116639. doi:10.1016/j.bcp.2024.116639
- Liu R, Wang Y, Kuai W, et al. Troxerutin suppress inflammation response and oxidative stress in jellyfish dermatitis by activating Nrf2/HO-1 signaling pathway. *Front Immunol.* 2024;15:1369849. doi:10.3389/fimmu.2024.1369849
- Li J, Wang T, Liu P, et al. Hesperetin ameliorates hepatic oxidative stress and inflammation via the PI3K/AKT-Nrf2-ARE pathway in oleic acid-induced HepG2 cells and a rat model of high-fat diet-induced NAFLD. *Food Funct.* 2021;12(9):3898–3918. doi:10.1039/d0fo02736g
- Cao TY, Qu HH, Dong LY, et al. Preventive and protective effects of Jingfang Granules on aristolochic acid induced acute kidney injury in mice. *Chin Traditional Herbal Drugs.* 2022;53(18):5742–5749.
- Dong LY, Cheng GL, Yao JC, et al. Protective effect of Jingfang Granules on acute myocardial infarction induced by isoproterenol in rats. *Chin Traditional Herbal Drugs.* 2022;53(21):6785–6794.
- Li SR, Wu JY, Cao NN, et al. Jingfang granules ameliorate inflammation and immune disorders in mice exposed to low temperature and high humidity by restoring the dysregulation of gut microbiota and fecal metabolites. *Biomed Pharmacother.* 2023;165:115050. doi:10.1016/j.biopha.2023.115050
- Xu JX, Zhang MJ, Wang AR, Li LM, Gu ML, Li SK. Clinical application of Jingfang Baidu San Jiawei combined with auricular acupuncture in prophylaxis and treatment of epidermal growth factor receptor inhibitor related skin toxicity. *Chin Arch Tradit Chin Med.* 2018;36(2). doi:10.13193/j.issn.1673-7717.2018.02.042
- Xu JN, Duan LH. Experiences in the treatment of acne with modified Jing Fang Bai Du San. *World J Integr Tradit West Med.* 2016;11(10):1451–1453+1460. doi:10.13935/j.cnki.sjzx.161033
- Xu QQ, Sheng LS, Zhu X, et al. Jingfang granules exert anti-psoriasis effect by targeting MAPK-mediated dendritic cell maturation and PPAR $\gamma$ -mediated keratinocytes cell cycle progression in vitro and in vivo. *Phytomedicine.* 2023;117:154925. doi:10.1016/j.phymed.2023.154925
- Sun CH, Liang HB, Zhao Y, et al. Jingfang Granules improve glucose metabolism disturbance and inflammation in mice with urticaria by up-regulating LKB1/AMPK/SIRT1 axis. *J Ethnopharmacol.* 2023;302(Pt A):115913. doi:10.1016/j.jep.2022.115913
- Sun B, Lin L, Yao T, et al. Jingfang Granule mitigates coxsackievirus B3-induced myocardial damage by modulating muclolipin 1 expression. *J Ethnopharmacol.* 2024;320:117396. doi:10.1016/j.jep.2023.117396
- Lu X, Liu M, Dong H, Miao J, Stagos D, Liu M. Dietary prenylated flavonoid xanthohumol alleviates oxidative damage and accelerates diabetic wound healing via Nrf2 activation. *Food Chem Toxicol.* 2022;160:112813. doi:10.1016/j.fct.2022.112813
- Guo M, Wang R, Geng J, et al. Human TFF2-Fc fusion protein alleviates DSS-induced ulcerative colitis in C57BL/6 mice by promoting intestinal epithelial cells repair and inhibiting macrophage inflammation. *Inflammopharmacol.* 2023;31(3):1387–1404. doi:10.1007/s10787-023-01226-9
- Lu X, Qin L, Guo M, et al. A novel alginate from *Sargassum* seaweed promotes diabetic wound healing by regulating oxidative stress and angiogenesis. *Carbohydr Polym.* 2022;289:119437. doi:10.1016/j.carbpol.2022.119437
- Ghasemi A, Jeddi S. Streptozotocin as a tool for induction of rat models of diabetes: a practical guide. *EXCLI J.* 2023;22:274–294. doi:10.17179/excli2022-5720
- Sun XX, Xiang HX, Liu Z, et al. Jingfang Granules alleviates bleomycin-induced acute lung injury through regulating PI3K/Akt/mTOR signaling pathway. *J Ethnopharmacol.* 2024;318(Pt A):116946. doi:10.1016/j.jep.2023.116946
- Hsin KY, Ghosh S, Kitano H. Combining machine learning systems and multiple docking simulation packages to improve docking prediction reliability for network pharmacology. *PLoS One.* 2013;8(12):e83922. doi:10.1371/journal.pone.0083922

29. Heo SJ, Hwang JY, Choi JI, et al. Protective effect of diphlorethohydroxycarmalol isolated from *Ishige okamurae* against high glucose-induced-oxidative stress in human umbilical vein endothelial cells. *Food Chem Toxicol.* 2010;48(6):1448–1454. doi:10.1016/j.fct.2010.02.025
30. Okonkwo UA, DiPietro LA. Diabetes and wound angiogenesis. *Int J Mol Sci.* 2017;18(7):1419. doi:10.3390/ijms18071419
31. Duraisamy Y, Slevin M, Smith N, et al. Effect of glycation on basic fibroblast growth factor induced angiogenesis and activation of associated signal transduction pathways in vascular endothelial cells: possible relevance to wound healing in diabetes. *Angiogenesis.* 2001;4(4):277–288. doi:10.1023/a:1016068917266
32. Liu DG, Zhao WX, Xu Y, et al. Protective effect of Jingfang Granules on retina of diabetic mice. *Chin Tradit Herbal Drug.* 2024;55(09):2996–3005. doi:10.7501/j.issn.0253-2670.2024.09.014
33. Sharifiaghdam M, Shaabani E, Faridi-Majidi R, De Smedt SC, Braeckmans K, Fraire JC. Macrophages as a therapeutic target to promote diabetic wound healing. *Mol Ther.* 2022;30(9):2891–2908. doi:10.1016/j.ymthe.2022.07.016
34. Jie L, Ming Z, Yan-yan W. Molecular biological mechanism of diabetic foot. *Chin J Tissue Eng Res.* 2006;12:142–144.
35. Wallace LA, Gwynne L, Jenkins T. Challenges and opportunities of pH in chronic wounds. *Ther Deliv.* 2019;10(11):719–735. doi:10.4155/tde-2019-0066
36. Sim P, Strudwick XL, Song Y, Cowin AJ, Garg S. Influence of acidic pH on wound healing in vivo: a novel perspective for wound treatment. *Int J Mol Sci.* 2022;23(21):13655. doi:10.3390/ijms232113655
37. Zhao G, Usui ML, Lippman SI, et al. Biofilms and inflammation in chronic wounds. *Adv Wound Care.* 2013;2(7):389–399. doi:10.1089/wound.2012.0381
38. Xu J, Wang E, Yu L, Zhang W, Sun Y, Zhang G. Toxicity of Jingfang granule extract by repeated gavage for 28 days in young rats. *Chin J Pharmacovigil.* 2022;19(05):515–521. doi:10.19803/j.1672-8629.2022.05.09
39. Yang D, Qu Y, Zhu Q, et al. Randomized double-blind placebo-controlled trial of Jingfang Granules in treatment of common cold (wind-cold syndrome). *China J Chinese Materia Medica.* 2022;47(10):2819–2824. doi:10.19540/j.cnki.cjcmm.20220209.501
40. Ni W, Tang H, Sun C, Yao J, Zhang X, Zhang G. Inhibitory effect of Jingfang mixture on *Staphylococcus aureus* alpha-hemolysin. *World J Microbiol Biotechnol.* 2024;40(9):286. doi:10.1007/s11274-024-04073-0
41. Chen BN, Zhao Q, Ni R, et al. Inhibition of calpain reduces oxidative stress and attenuates endothelial dysfunction in diabetes. *Cardiovasc Diabetol.* 2014;13(88). doi:10.1186/1475-2840-13-88
42. Wang Y, Graves DT. Keratinocyte function in normal and diabetic wounds and modulation by FOXO1. *J Diabetes Res.* 2020;2020:3714704. doi:10.1155/2020/3714704
43. Geng XY, Wang Y, Li H, et al. Total iridoid glycoside extract of *lamiophlomis rotata* (Benth) kudo accelerates diabetic wound healing by the NRF2/COX2 axis. *Chin Med.* 2024;19(1). doi:10.1186/s13020-024-00921-1
44. Li M, Hou Q, Zhong L, Zhao Y, Fu X. Macrophage related chronic inflammation in non-healing wounds. *Front Immunol.* 2021;12:681710. doi:10.3389/fimmu.2021.681710
45. Lin CW, Hung CM, Chen WJ, et al. New horizons of macrophage immunomodulation in the healing of diabetic foot ulcers. *Pharmaceutics.* 2022;14(10):2065. doi:10.3390/pharmaceutics14102065
46. Chang M, Nguyen TT. Strategy for treatment of infected diabetic foot ulcers. *Acc Chem Res.* 2021;54(5):1080–1093. doi:10.1021/acs.accounts.0c00864
47. Liu C, Hu F, Jiao G, et al. Dental pulp stem cell-derived exosomes suppress M1 macrophage polarization through the ROS-MAPK-NFkappaB P65 signaling pathway after spinal cord injury. *J Nanobiotechnology.* 2022;20(1):65. doi:10.1186/s12951-022-01273-4
48. Medicherla S, Wadsworth S, Cullen B, et al. p38 MAPK inhibition reduces diabetes-induced impairment of wound healing. *Diabetes Metab Syndr Obes.* 2009;2:91–100. doi:10.2147/DMSO.S5859
49. Liu B, Yu CJ, Meng XB, et al. Effects of Qizhi Jiangtang capsule on dermal ulcer in type 2 diabetic rats. *China J Chin Materia Medica.* 2016;41(06):118–123. doi:10.4268/cjcmm20160123
50. Gauthier T, Yao C, Dowdy T, et al. TGF-beta uncouples glycolysis and inflammation in macrophages and controls survival during sepsis. *Sci Signal.* 2023;16(797):eade0385. doi:10.1126/scisignal.ade0385
51. Stothers CL, Burelbach KR, Owen AM, et al. Beta-glucan induces distinct and protective innate immune memory in differentiated macrophages. *J Immunol.* 2021;207(11):2785–2798. doi:10.4049/jimmunol.2100107
52. Zhang E, Gao B, Yang L, Wu XJ, Wang ZT. Notoginsenoside Ft1 promotes fibroblast proliferation via PI3K/Akt/mTOR signaling pathway and benefits wound healing in genetically diabetic mice. *J Pharmacol Exp Ther.* 2016;356(2):324–332. doi:10.1124/jpet.115.229369
53. Qu KS, Cha HJ, Ru Y, Que H, Xing M. Buxuhuyay decoction accelerates angiogenesis by activating the PI3K-Akt-eNOS signalling pathway in a streptozotocin-induced diabetic ulcer rat model. *J Ethnopharmacol.* 2021;273:113824. doi:10.1016/j.jep.2021.113824
54. Qin PY, Xu YJ, Zuo XD, et al. Effect and mechanisms of polygonatum kingianum (polygonati rhizome) on wound healing in diabetic rats. *J Ethnopharmacol.* 2022;298. doi:10.1016/j.jep.2022.115612
55. Song M, Chen L, Li CX, et al. Effect of Naoxintong capsule on wound healing in typeII diabetic mice. *J Tianjin University Tradit Chin Med.* 2019;38(04):406–411. doi:10.11656/j.issn.1673-9043.2019.04.21
56. Li H, Liang J, Li P, et al. *Schizonepeta tenuifolia* Briq-Saposhnikovia divaricata decoction alleviates atopic dermatitis via downregulating macrophage TRPV1. *Front Pharmacol.* 2024;15:1413513. doi:10.3389/fphar.2024.1413513
57. Zhu H, Liu J, Zhou J, et al. Notopterygium incisum roots extract (NRE) alleviates neuroinflammation pathology in Alzheimer's disease through TLR4-NF-kappaB pathway. *J Ethnopharmacol.* 2024;335:118651. doi:10.1016/j.jep.2024.118651
58. Zhao L, Chen X, Shao X, et al. Prenylated phenolic compounds from licorice (*Glycyrrhiza uralensis*) and their anti-inflammatory activity against osteoarthritis. *Food Funct.* 2022;13(2):795–805. doi:10.1039/d1fo03659a
59. Yuan Q, Zhang J, Xiao C, et al. Structural characterization of a low-molecular-weight polysaccharide from *Angelica pubescens maxim. f. biserrata* Shan et Yuan root and evaluation of its antioxidant activity. *Carbohydr Polym.* 2020;236:116047. doi:10.1016/j.carbpol.2020.116047
60. Feng A, Zhao Z, Liu C, et al. Study on characterization of *Bupleurum chinense* polysaccharides with antioxidant mechanisms focus on ROS relative signaling pathways and anti-aging evaluation in vivo model. *Int J Biol Macromol.* 2024;266(Pt 2):131171. doi:10.1016/j.ijbiomac.2024.131171
61. Pasandideh S, Arasteh A. Evaluation of antioxidant and inhibitory properties of citrus aurantium L. on the acetylcholinesterase activity and the production of amyloid nano-bio fibrils. *Int J Biol Macromol.* 2021;182:366–372. doi:10.1016/j.ijbiomac.2021.04.043

62. Wang S, Liu Y, Wang X, et al. Modulating macrophage phenotype for accelerated wound healing with chlorogenic acid-loaded nanocomposite hydrogel. *J Control Release*. 2024;369:420–443. doi:10.1016/j.jconrel.2024.03.054
63. Li K, Wu L, Jiang J. Apigenin accelerates wound healing in diabetic mice by promoting macrophage M2-type polarization via increasing miR-21 expression. *Mol Cell Biochem*. 2024;479(11):3119–3127. doi:10.1007/s11010-023-04885-y
64. Han Z, Li A, Xue Z, Guan SB, Yin G, Zheng X. Eugenol-loaded polyurethane gelatin dressing for efficient angiogenesis and antibacterial effects in refractory diabetic wound defect healing. *Int J Biol Macromol*. 2024;271(Pt 2):132619. doi:10.1016/j.ijbiomac.2024.132619
65. Sun M, Xie Q, Cai X, et al. Preparation and characterization of epigallocatechin gallate, ascorbic acid, gelatin, chitosan nanoparticles and their beneficial effect on wound healing of diabetic mice. *Int J Biol Macromol*. 2020;148:777–784. doi:10.1016/j.ijbiomac.2020.01.198

## Drug Design, Development and Therapy

### Publish your work in this journal

Drug Design, Development and Therapy is an international, peer-reviewed open-access journal that spans the spectrum of drug design and development through to clinical applications. Clinical outcomes, patient safety, and programs for the development and effective, safe, and sustained use of medicines are a feature of the journal, which has also been accepted for indexing on PubMed Central. The manuscript management system is completely online and includes a very quick and fair peer-review system, which is all easy to use. Visit <http://www.dovepress.com/testimonials.php> to read real quotes from published authors.

Submit your manuscript here: <https://www.dovepress.com/drug-design-development-and-therapy-journal>

**Dovepress**

Taylor & Francis Group